DISTRIBUTED CONTROL OF AN AUTONOMOUS WHEELCHAIR USING STEADY STATE VISUAL EVOKED POTENTIAL BASED BRAIN COMPUTER INTERFACE

DANNY NG WEE KIAT

DOCTOR OF PHILOSOPHY (ENGINEERING)

LEE KONG CHIAN
FACULTY OF ENGINEERING AND SCIENCE
UNIVERSITI TUNKU ABDUL RAHMAN
JUNE 2021

DISTRIBUTED CONTROL OF AN AUTONOMOUS WHEELCHAIR USING STEADY STATE VISUAL EVOKED POTENTIAL BASED BRAIN COMPUTER INTERFACE

By

DANNY NG WEE KIAT

A thesis submitted to the Department of Mechanical and Materials
Engineering,

Lee Kong Chian Faculty of Engineering and Science,

Universiti Tunku Abdul Rahman,

in partial fulfilment of the requirements for the degree of

Doctor of Philosophy (Engineering)

June 2021

ABSTRACT

**DISTRIBUTED CONTROL OF AN AUTONOMOUS
WHEELCHAIR USING STEADY STATE VISUAL EVOKED
POTENTIAL BASED BRAIN COMPUTER INTERFACE**

Danny Ng Wee Kiat

Having the capability to control a wheelchair using brain signals would be a major benefit to patients suffering from motor disabling diseases. However, one major challenge facing such systems is the number of inputs needed over time by the patient for control. The objective of this study is to develop a "hybrid" system that requires less inputs from a subject to operate a wheelchair compared to the ones driven directly using BCI. A distributed control system using an autonomous wheelchair with inputs from a steady-state visual evoked potential-based brain-computer interface was developed to achieve the objective. A dual-mode system was implemented in this study to allow the autonomous wheelchair to work in both unknown and known environments. Such system is suitable for a person with physical and mobility impairments. The developed system required an average of 16.6 selections compared to a BCI wheelchair with direct control where an average of 32.8 selections was needed to complete a navigation task in this study. The lower number of required inputs reduces the number of mental tasks by the subjects. This is the first system that incorporates robotic and BCI to control a wheelchair, relegating the responsibility of navigation control from the subjects to the navigation software.

ACKNOWLEDGEMENTS

APPROVAL SHEET

This thesis entitled **'DISTRIBUTED CONTROL OF AN AUTONOMOUS WHEELCHAIR USING STEADY STATE VISUAL EVOKED POTENTIAL BASED BRAIN COMPUTER INTERFACE'** was prepared by DANNY NG WEE KIAT and submitted as partial fulfilment of the requirement for the degree of Doctor of Philosophy (Engineering) at Universiti Tunku Abdul Rahman.

Approved by:

_____

(Prof. Dato' Dr Goh Sing Yau)   Date: 28 June 2021
Supervisor
Department of Mechanical and Material Engineering
Lee Kong Chian Faculty of Engineering and Science
Universiti Tunku Abdul Rahman

_____

(Dr. Mok Siew Ying)   Date: 28 June 2021
Co-Supervisor
Department of Mechanical and Material Engineering
Lee Kong Chian Faculty of Engineering and Science
Universiti Tunku Abdul Rahman

LEE KONG CHIAN FACULTY OF ENGINEERING AND SCIENCE

UNIVERSITI TUNKU ABDUL RAHMAN

Date: 28 June 2021

SUBMISSION OF THESIS

It is hereby certified that **DANNY NG WEE KIAT** (ID No: **13UED02777**) has completed this thesis entitled "**DISTRIBUTED CONTROL OF AN AUTONOMOUS WHEELCHAIR USING STEADY STATE VISUAL EVOKED POTENTIAL BASED BRAIN COMPUTER INTERFACE**" under the supervision of Prof. Dato' Dr. Goh Sing Yau (Supervisor) from the Department of Mechanical and Material Engineering, Lee Kong Chian Faculty of Engineering and Science (LKC FES), and Dr Mok Siew Ying (Co-Supervisor) from the Department of Biomedical and Mechatronic Engineering, Lee Kong Chian Faculty of Engineering and Science (LKC FES).

I understand that University will upload softcopy of my thesis in pdf format into UTAR Institutional Repository, which may be made accessible to UTAR community and public.

Yours truly,

_____
(DANNY NG WEE KIAT)

DECLARATION

I hereby declare that the dissertation is based on my original work except for quotations and citations which have been duly acknowledged. I also declare that it has not been previously or concurrently submitted for any other degree at UTAR or other institutions.

Name   Danny Ng Wee Kiat

Date   28 June 2021

TABLE OF CONTENTS

LIST OF TABLES

LIST OF FIGURES

LIST OF ABBREVIATIONS

AMCL	Adaptive Monte Carlo Localization
BCI	Brain-Computer Interface
ECoG	Electrocorticographic
EEG	Electroencephalogram
ERD	Event-Related Desynchronization
ERS	Event-Related Desynchronization
FFT	Fast Fourier Transform
fNIRS	Functional Near-Infrared Spectroscopy
IMU	Inertia Measurement Unit
LCD	Liquid Crystal Display
LED	Light Emitting Diode
MI	Motor Imagery
PCB	Printed Circuit Board
PGA	Programmable Gain Amplifier
ROS	Robot Operating System
SLAM	Simultaneous Localization and Mapping
SPI	Serial Peripheral Interface
SSVEP	Steady-State Visual Evoke Potential
TEB	Time Elastic Band
UART	Universal Asynchronous Receiver Transmitter
USB	Universal Serial Bus
VEP	Visual Evoke Potential

CHAPTER 1

INTRODUCTION

1.1 Brain-Computer Interface

A Brain-computer Interface (BCI) is a type of human-computer interaction where a pathway is formed between the human brain to the computer for control and communication (Wolpaw, et al., 2002). Some of the common methods to capture brain signals are electroencephalography (EEG), (Pfurtscheller & Neuper, 2001), functional near-infrared spectroscopy (fNIRS), (Ito, et al., 2013) or electrocorticography (ECoG) (Fifer, et al., 2013). Features extracted from the captured brain signals can be used as inputs for the BCI. Steady-state visual evoked potential (SSVEP) or event-related potential (ERP) such as P300 and motor imagery signals are some examples of brain signals used as inputs to a BCI. Software algorithms to capture, process, extract and classify these signals were the focus of numerous studies (Ramadan & Vasilakos, 2017; Blankertz, et al., 2011; Li, et al., 2011; Lotte, et al., 2018). The algorithms can associate these classified features to specific inputs in the developed applications. The BCI enables a person to convey commands to the computer without physical interactions.

1.2 Application of BCI

Multiple applications in communication (Yu, et al., 2017; Wolpaw, et al., 2018), robotics (Leeb, et al., 2015; Zhang, et al., 2017), prosthetics (Muller-Putz & Pfurtscheller, 2008; Goh, et al., 2005), and rehabilitation (Bockbrader, et al.,

2018) were developed using BCI as the control methods in recent years. These studies show the promising potential in the utilization of BCI technology as a means of control. The BCI is proven to be very useful for a person with physical and mobility impairments to interact with a computer.

Wheelchair control using BCIs is one of the areas where studies were conducted by numerous researchers. BCIs utilizing signals such as steady-state visual evoked potential (SSVEP), P300, motor imagery signal, or hybrid signals are applied as the means to control the wheelchairs (Fernández-Rodríguez, et al., 2016).These signals are mapped to specific commands such as a destination (Ng, et al., 2014) or direction (Muller-Putz & Pfurtscheller, 2008) for the control of the wheelchair. A BCI-controlled wheelchair allows a person with physical and mobility impairments to control a wheelchair without physical interactions. This is important as a study by Kübler (Kübler, et al., 2005)shows that freedom, defined as the capability to move around without assistance, as the third relevant aspect that affects the quality of life after relationship and health for a patient with amyotrophic lateral sclerosis (ALS). The BCI is a very powerful tool that allows a person to regain independence for mobility.

However, the BCI is a complex system where training is needed to ensure that the users can operate the system as intended (Thompson, 2019).Besides this, mental fatigue is another problem faced by users of a BCI system. An increase in mental load and fatigue was observed when the users were stimulated by a continuous flickering light stimulus (Xie, et al., 2016)when using a SSVEP-based BCI system. A slight decrease in the quality of SSVEP response was observed during long-time usage of the BCI system (Seo, et al.,

2019). These problems affect the classification accuracy of the BCI causing an issue for users to pass valid commands to the computer.

1.3 Motivation and Research Objective

A BCI system has its limitation when the user needs to operate the system for a long time or needs to issue multiple commands in succession despite having the advantage of being an interface that operates without physical interactions. It is important to address this issue for the BCI system. This study focused on the application of BCI for the control of a wheelchair as the ability for a person with physical and mobility impairments to be able to move independently is important.

The objective of this study is to develop a "hybrid" system that requires less inputs from a subject to operate the BCI wheelchair compared to the ones driven directly using BCI. There are two specific requirements that the developed wheelchair need to fulfil in order to achieve this objective. The first is a BCI system that can capture EEG signals and classify SSVEP. The classified SSVEP will act as the trigger to move the wheelchair. The second is the capability to control the wheelchair independent of the BCI system. This can be achieved through the development of a distributed control system using an autonomous wheelchair. Techniques from robotic systems will be incorporated into the wheelchair for autonomous movements. Experiments will be conducted on the wheelchair to study the operation of the developed wheelchair in an indoor environment.

1.4   Thesis Overview

There are five chapters in this thesis. Chapter 1 gives a short introduction to the overview, applications, pros, and cons of a BCI system. The motivation and research objective are included in the last part of this chapter. Chapter 2 contains the literature survey of SSVEP-based BCI systems and their applications. The use of robotics techniques in wheelchair systems is also discussed in this chapter. Chapter 3 focuses on the methodology used in the design of this wheelchair. This chapter explains the algorithm, technique, and device developed for this study. Chapter 4 provides the results and discussions on the experiments conducted to test the operation of the developed autonomous wheelchair in an indoor environment. Chapter 5 summarises and concludes the finding of this study. Future recommendations for future works are also given in this chapter.

CHAPTER 2

LITERATURE REVIEW

2.1   Introduction

This chapter starts with a review of SSVEP-based BCI. The application of SSVEP for BCI with its pros and cons are discussed next. After that, a review is conducted on the implementation of BCI for the control of the wheelchair. Lastly, the application of robotic techniques on a wheelchair was reviewed and discussed.

2.2   SSVEP-based BCI

Evoked potentials are detectable changes of electrical activity in the brain triggered by sensory stimuli. Adrian & Matthews (1934) were the first to show that rhythmic potential changes can be detected from the occipital region when a subject was stimulated by bright flickering lights (Adrian & Matthews, 1934). In the study, flickering lights between 8Hz and 24Hz were used and the corresponding electrical potential was recorded. This study described the SSVEP phenomena where the frequency of brain electrical potentials recorded was like the frequency of stimulus shown to the subjects. Since the discovery, SSVEP became the focus of a wide variety of scientific studies and applications (Norcia, et al., 2015).

A typical setup for SSVEP-based BCI consists of a device to generate light stimulus, an EEG acquisition unit, the computer algorithms to interpret the acquired signals and to control external devices as needed by the applications

(Zhang, et al., 2019).Figure 2.1 shows an example of a typical SSVEP-based BCI setup. Source of flickering lights are used to elicit SSVEP response in the subject. The study by Herrmann (2001) showed that the frequency of SSVEP can be detected for stimulus frequency up to 90Hz (Herrmann, 2001). Computer monitors and light emitting diode (LED) are common devices used to generate flickering lights (Zhu, et al., 2010). The range of frequencies that can be generated on a computer screen is lower than the LEDs. Computer monitors have a usual refresh rate of 60Hz limiting the stimulus frequencies to be below 30Hz. LED can be used to generate any frequencies for stimulus. However, extra electronic components and control circuitry are required.
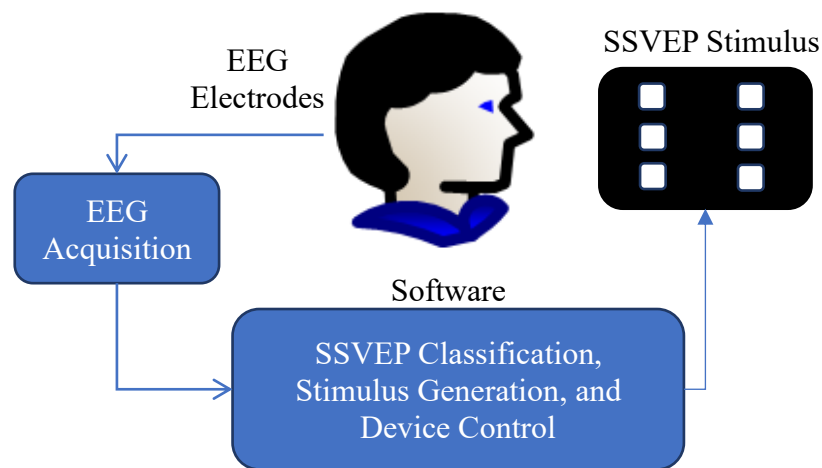
Figure 2.1:   Typical setup of a SSVEP-based BCI system. The three main parts of a SSVEP-based BCI are the source of stimulus, the EEG acquisition unit, and the software for the BCI.

Besides frequency information, phase information can also be obtained from SSVEP. Study by Wilson et al. (2014) had shown that phase information can be obtained from SSVEP signals if the duty cycle of the stimulus is varied. It is also worth noting that the colour of the light stimulus will affect the performance of SSVEP. A Previous study showed that white colour stimulus led

to the best performance (Cao, 2012).

The next component in the SSVEP-based BCI is the EEG acquisition unit. EEG signals from the occipital lobe will be captured by the EEG acquisition unit. Measurements are taken from electrodes are placed on the occipital region according to the 10-20 system. Figure 2.2 shows the placement of electrodes according to the 10-20 system. There are five types of electrodes for the measurement of EEG, which are disposable electrodes, reusable electrodes, cup electrodes, saline-based electrodes, and needle electrodes (Teplan, 2002). High impedance at the site of measurements will lead to noisy EEG recording. Conductive gel and skin abrasive are used at the site of measurement to achieve low impedance. The amplitude of EEG potentials is in the range of 10μV to 100μV (Aurlien, et al., 2004). Amplification and signal conditioning are implemented in this step to prepare the signals for digital conversion by the acquisition unit (Teplan, 2002). Amplifiers having high common-mode rejection ratio is important for EEG amplifiers (Texas Instruments, 2017). This is to ensure that the noise that is present on each of the electrode is attenuated by the amplifiers. It is important to obtain a good signal-to-noise ratio of the measured EEG as the presence of noise in the signal might affect the accuracy of the classification software. Once the EEG signals are digitized, the signals can be transmitted to the computer for further processing. Another aspect that is important for an EEG acquisition unit is the safety of the device. The EEG acquisition unit creates a low impedance connection to the human body. It is therefore important to ensure that the leakage current from the device does not harm the users of the EEG acquisition unit (Webster, 1998).
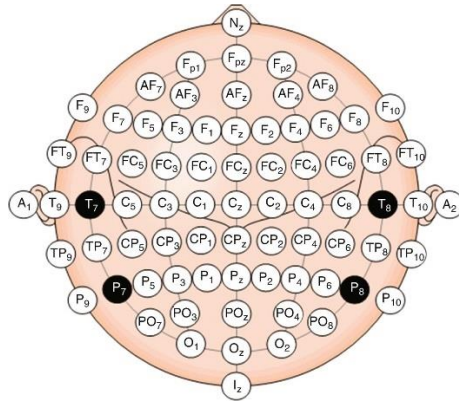
Figure 2.2:   10-20 EEG System placement system (Sazgar & Young, 2019). PO and O are the electrode positions where the measurements of EEG signals from the occipital lobe of the brain can be made.
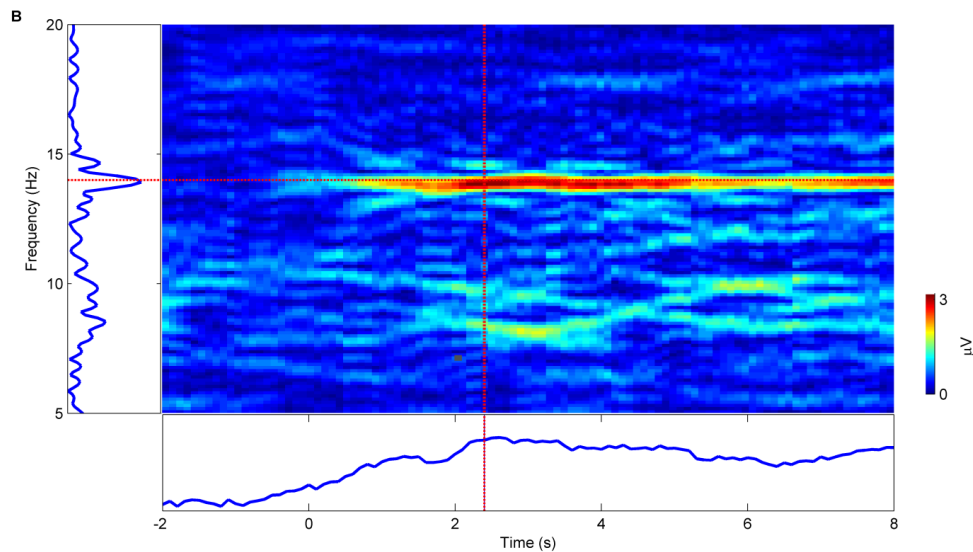
Figure 2.3:   SSVEP spectrogram obtained from a subject looking at a 15Hz stimulus evoked by stimulators generated on a Liquid Crystal Display (LCD) monitor (Mah, et al., 2019).SSVEP response of 15Hz (red area) can be observed from the captured signals.

Once transmitted to the computer, further signal processing such as filtering and Fast Fourier Transform (FFT) can be performed on the acquired EEG. Digital filters such as notch filters and bandpass filters can be implemented in the software to remove movement artifacts and powerline noise (Widmann, et al., 2015). EEG spectrogram can be obtained by performing short-time Fourier transform of the EEG signals. The spectrogram can show the

changes in the frequency component of the measured signals over time. Figure 2.3 shows an example of a spectrogram where SSVEP is present. The EEG spectrogram gives a visual representation of brainwave measured in the frequency domain over time, allowing for easy identification of SSVEP through visual inspection.

BCI software algorithms to extract features and classifiers were developed to automatically classify SSVEP. Features extractions methods such as power spectrum density analysis (PSDA) using Fourier transform, Wavelet transform and Hilbert-Huang transform (HHT) were implemented to extract SSVEP features from the recorded brain signals (Liu, et al., 2014). These methods work by decomposing the recorded EEG signals into simpler components. Fourier Transform decomposes the recorded signals into weighted sums of sinusoidal signals giving information on the contribution of individual frequency towards the signal. Wavelet transforms decompose the signals into a set of basis functions (wavelet) (Daubechies, 1990). The wavelet component containing the frequency of interest can be extracted as a feature. HHT decomposes the signals into intrinsic mode functions (Boashash, 2015). These functions represent the local characteristics of non-stationary signals. PSDA extracted using FFT is one of the common features used in other studies (Al-maqtari, et al., 2009; Diez, et al., 2011; Diez, et al., 2013; Cheng, et al., 2002; Hwang, et al., 2012; Muller-Putz & Pfurtscheller, 2008; Wang, et al., 2010) for SSVEP-based BCI due to the simplicity of the FFT algorithm. After feature extractions, feature classification needs to be conducted to classify the signals for SSVEP. Value thresholding and classifier such as Linear Discriminant

Analysis (LDA), Linear Fisher classifier, or Support Vector Machine are the two common methods used for SSVEP (Liu, et al., 2014). Value thresholding such as the power of the intended frequency (Cheng, et al., 2002), or the dwell time of the subject on the stimulus (Muller-Putz & Pfurtscheller, 2008) is used to detect SSVEP. Once the classification is successful, the chosen SSVEP feature can be correlated to a pre-set function in the BCI application.

One area of application for SSVEP-based BCI is in communication. BCI spelling system where a QWERTY style keyboard with flickering LED lights was developed for the users to type with (Hwang, et al., 2012). This enables the user to interact with a computer using existing interfaces such as a QWERTY keyboard. There are also simplified forms of communication such as SSVEP selection of pictures and phrases (Dehzangi & Farooq, 2018). These simplify the communications and categorize them into a set of preselected phrases that the users can convey. Another area of application for SSVEP-based BCI is for the control of a prosthetic arm. SSVEP was used to control the axis of motion for a robotic arm in one of the studies conducted (Muller-Putz & Pfurtscheller, 2008). SSVEP-based target control of the robotic arm was also implemented in another study (Chen, et al., 2018). In the study, SSVEP was used to select one of the 15 pre-set targets in the software for the robotic arm to move to. SSVEP-based BCI was also used to control an avatar in a virtual environment where the user's avatar can navigate around the environment (Faller, et al., 2010) allowing for social interaction in a virtual environment. Similarly, for social interaction, a SSVEP-based BCI was used to control the gesture of a telepresence robot (Kishore, et al., 2014). All these applications show the usefulness of SSVEP as

a means of input for different applications.

2.3 BCI Controlled System

One of the earliest published studies on BCI wheelchairs was conducted by Tanaka et al. (2005) (Tanaka, et al., 2005). In the study, the subjects were tasked with thinking of moving left or right to drive the wheelchair to the left or right goal. Since then, there are numerous studies on BCI wheelchairs using different types of brain signals, navigation, and control systems (Fernández-Rodríguez, et al., 2016).
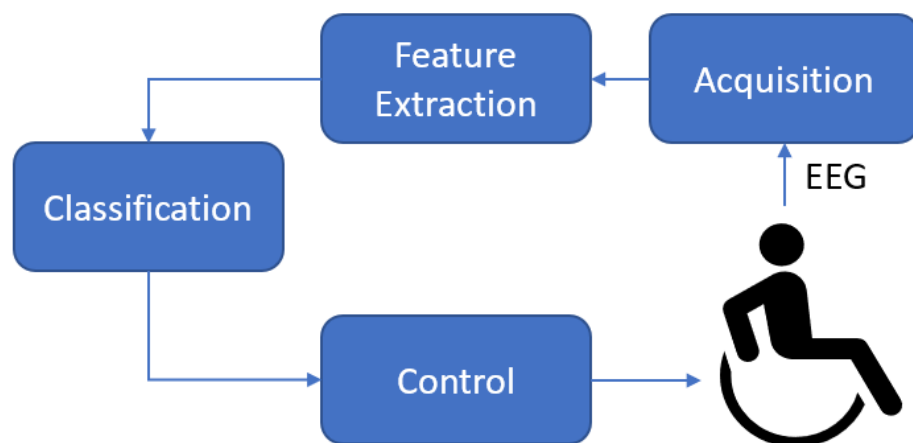
Figure 2.4   Block diagram of a BCI wheelchair. EEG is captured from the subject by the acquisition system using electrodes. Raw EEG signals are analysed to get features for classification. The classification algorithm will determine the state of the EEG signals captured. After classification, the system will trigger the software to move the wheelchair.

Figure 2.4 shows a block diagram of how BCI wheelchair functions. All studies that are reviewed later in this section have a similar system as shown by the block diagram in Figure 2.4. EEG features such as Event-Related Desynchronization (ERD) and Event-Related Desynchronization (ERS)

triggered by Motor Imagery (MI) (Tanaka, et al., 2005; Millan, et al., 2009), P300 (Rebsamen, et al., 2007; Iturrate, et al., 2009), and SSVEP (Mandel, et al., 2009; Xu, et al., 2012). The classification method implemented in the studies depends on the EEG feature selected. The classifier developed by Tanaka et al. (2005) used FFT features classified using pattern recognition trained by a recursive training algorithm. For P300, EEG features in the time domain were used for classification. Classifier methods such as linear discriminant analysis (Iturrate, et al., 2009) or support vector machine (Rebsamen, et al., 2007) were used for P300. For SSVEP, EEG features in the frequency domain such as amplitude extracted using FFT (Mandel, et al., 2009) or canonical correlation analysis coefficient (Xu, et al., 2012) was used for classification. Depending on the feature used, classification of SSVEP was conducted by using thresholding (Mandel, et al., 2009) or Bayesian classifier (Xu, et al., 2012). Besides these methods, the peak frequency in an EEG window was also used for the classification of SSVEP (Müller, et al., 2013).

Once the classification stage is completed, the software will issue commands for the wheelchair to move. Depending on the EEG features and classification used, the control of the wheelchairs can be of discrete commands or continuous control (Fernández-Rodríguez, et al., 2016). Discrete controls present the users with a choice for motion, for example, the choice to move forward/backward, left/right, or stop at a prefixed distance or angle (Varona-Moya, et al., 2015).Continuous control gives the users the ability to control the movement of the wheelchair directly, for example, the duration of turning or the acceleration of the wheelchair using BCI (Li, et al., 2014). A BCI-controlled

wheelchair allows for the control of a wheelchair using brain signals only without the need for physical control.

Shared-control BCI is one of the techniques that previous researchers had demonstrated in the control of robotics system. A study by Chung et al. (2011) demonstrated the use of a hierarchical architecture BCI for the control of a humanoid robot. In this architecture the user of the system can teach the robot new tasks using the SSVEP-based BCI. Comparison was done by the researcher to show the reduction of SSVEP tasks required to control the robot using the hierarchical architecture. Another example of the shared-control system was the use of BCI and vision systems for robotic arm control (Tang, 2017). In this system, machine vision was used to identify the potential targets for the robotic arm that were then used as selection choices by the BCI system. Another study also showed the use of share control of BCI system in the telepresence robot (Tonin, 2010). In this study, a low-level obstacle avoidance system was included in the telepresence robot. This allowed the subject to drive the telepresence robot around using BCI without hitting into obstacles. All These studies showed that it is possible to increase the usability of a BCI system through the addition of techniques from other fields of study such as robotics, machine vision and user interface design.

Patients suffering from Amyotrophic Lateral Sclerosis (ALS), neuromuscular disorder or spinal cord injuries would benefit from a BCI-controlled system. These patients have difficulties in moving their muscles to complete their daily tasks. System such as BCI spellers (Massari, 2013) was developed to help ALS patients to communicate with the outside world. Li et al. (2014) developed a direct control BCI wheelchair for spinal cord injury patients. Do et al. (2013) developed a motor-imagery BCI system to control a robotic leg orthosis. These studies demonstrated some use case of a BCI system to assist patients for communication and mobility.

2.4 Smart wheelchair

One challenge when controlling a powered wheelchair for a person with physical and mobility impairments is the difficulty to perform specific manoeuvres on the wheelchair (Torkia, et al., 2015). BCI wheelchairs with a low number of inputs and slow control presents a challenge for the users when the wheelchair requires precise control to navigate through a confined area or an area with a high amount of foot traffic. One solution that previous studies explored is the integration of navigation techniques from other robotic applications for use with the wheelchair (Cruz, et al., 2010).

A smart wheelchair integrates a powered wheelchair with sensors, navigation algorithms, and intelligent control algorithms to achieve autonomous navigation (Simpson, 2005). Sensors such as depth cameras, ultrasonic range sensors, laser range finders, and inertial measurement units (IMU) were incorporated into smart wheelchairs (Rockey, et al., 2013). Depth cameras can

provide images as well as depth information of objects in the field of view of the camera that are useful for the autonomous navigation of a smart wheelchair (Li, et al., 2017). The 2D laser range finder is another common sensor used for smart wheelchairs (He, et al., 2017; Grewal, et al., 2017). The 2D laser range finder provides accurate distance measurements with high angular resolution. Another sensor that was used on smart wheelchairs is the ultrasonic range finders (Tan, et al., 2008; Punsawad & Wongsawat, 2013). Ultrasonic range finders can only provide measurement for the nearest object in its field of view. Although the resolution is the lowest compared to the depth camera and laser range finder, the ultrasonic range finder is still applied in smart wheelchairs because of its low cost (Rockey, et al., 2013). The IMU measures the angular rotation and acceleration of the wheelchair. Measurements obtained from the IMU can be used for dead reckoning calculations to localize the wheelchair (Khan, 2012). These sensors enable the wheelchair to perceive the surrounding, allowing the navigation algorithms to conduct path planning and to navigate while avoiding obstacles.

Simultaneous localization and mapping (SLAM) techniques enable the generation of a map from measurements obtained by sensors (Tsubouchi, 2019) attached to the wheelchair. The ability to generate maps using SLAM allows the wheelchair to plan for navigation beyond the sensing range of attached sensors. Global path planning can be conducted by the software of the wheelchair with the generated map (Koubaa, et al., 2018). Algorithms such as A* and Dijkstra's algorithm (Zhang & Zhao, 2014) can be implemented for global path planning once the map is generated. Local path planning with collision avoidance can be

implemented when the wheelchair is on route to the destination determined by the global path planner. Approaches such as Dynamic Window Approach (DWA), (Fox, et al., 1997) and Timed-Elastic-Band (TEB), (Rosmann, et al., 2013) can be implemented for local navigation. DWA conducts forward simulation based on the current location to predict the final location after a short period in the future. The optimal path is selected based on the trajectory generated by the DWA algorithm. TEB obtains the optimal trajectory by running sparse scalarized multi-objective optimization equations. Multiple trajectories are generated and optimized in parallel to select the optimal path to traverse. Both algorithms conduct planning with the latest sensor information. Once the algorithm is implemented, the wheelchair will be able to navigate to the destination while avoiding obstacles along the way.

2.5 Challenges in the implementation of a SSVEP-based BCI wheelchair

One of the challenges in the implementation of a BCI system is the complexity of the system. As reviewed above in Sections 2.1 and 2.2, there are multiple steps involved in the process of producing an action using a BCI system. Any misstep in any one of the processes involved will affect the accuracy of the BCI system. The quality of the recorded EEG, the generated stimuli and the effectiveness of the signal processing algorithm affect how well the system can classify the EEG event (Chabuda, et al., 2020). A study by Lee at al. (2019) (Lee, et al., 2019) conducted on 44 subjects where 38 subjects were first-time BCI users on the use of MI, ERP, and SSVEP found that only 15 subjects were able to control all three BCI paradigms proficiently. It is also noted in this study that

at least one type of BCI was usable by all the participants. This further complicates the implementation of BCI as more training was needed to increase proficiency in the usage of the system. Proper training protocols customized to individual users were needed to improve the usability of a BCI system (Thompson, 2019).

Besides, as mentioned in Section 1.2, mental fatigue is another problem faced by users of a BCI system. Subjects in the study conducted by Xie, et al. (2016) were required to perform 4 to 8 SSVEP BCI trials (Xie, et al., 2016). Each of the trial required the subject to focus on a stimulus for 5s for 20 times. There was a rest period of 5s between the stimulus. This study found that CCA results of the EEG signals recorded showed an offline accuracy of 74.33% ± 10.83 for fatigue level 4 state compared to the accuracy of 88.52% ± 11.07 for fatigue level 1 state. The study by Seo et al. (2019) found that there was a slight attenuation in the quality of SSVEP signals measured at the Oz location in the second session after subjects completed a session of ERP-, MI- and SSVEP-based BCI tasks. Changes in the signal amplitude due to fatigue may affect the accuracy of the system due to changes in the signal to noise ratio.

For a SSVEP-based BCI system, the number of distinct selections is limited by the size of the LCD monitor or the location of LED stimulators. Previous studies showed that the distance to the stimulus (Wu & Lakany, 2013) and the separation between the stimulus (Ng, et al., 2011) both affected the amplitude of SSVEP detected. This limits the number of choices a person can make when controlling the wheelchair with SSVEP. Another challenge in implementing the BCI wheelchair is the control of a moving wheelchair (Al-

qaysi, et al., 2018). Navigating a SSVEP wheelchair is a challenging task, involving making multiple control decisions in a dynamic environment. The wheelchair may pose a threat to the users or people nearby if unintended or wrong commands are issued by the users due to inappropriate use of the BCI.

2.6 Proposed design of a SSVEP-based BCI wheelchair

The challenges highlighted in Section 2.4 need to be overcome in the design of a SSVEP-based BCI wheelchair. The proposed wheelchair developed in this study will combine algorithms for navigation on a wheelchair with that for BCI-based SSVEP to reduce the number of inputs for control of BCI tasks. This is based on the idea of applying distributed controls for BCI applications initially explored by Goh et al. (Goh, et al., 2005) for the control of a prosthetic hand. The paper describes a prosthetic hand that has 4 fingers each with 3 segments and a thumb with 3 segments that can also rotate giving a total of 16 degrees of freedom. The hand movements were reduced to 4 main tasks – grab, pulp to pulp pinch, tripod pinch and key pinch so that the BCI only needs to provide one of four input selections to perform the desired task. The rest of the finger movements were carried out by a distributed controller.

Similarly, in the current study, it would require great mental effort by the user to provide the many successive inputs to move the wheelchair right, left, forward, backward or rotate and to avoid obstacles on the way to the destination. Instead, the task of controlling the motion of the wheelchair will be distributed to the navigation software for the wheelchair. The focus of the BCI will be to pass high-level commands such as one of several intended destinations to the

navigation software that will drive the wheelchair to the destination. More importantly, this approach will enable the incorporation of a safe controlled automatic emergency stop, without any intervention from the user, should a moving obstacle suddenly appear within the path of the wheelchair. In this context, the distributed wheelchair controller acts as a distributed controller, taking in the inputs from the sensors to make decision for navigation independent of the BCI system. The next chapter of this thesis will describe more details of the design of the SSVEP BCI autonomous wheelchair.

CHAPTER 3

DESIGN OF A SSVEP-BASED BCI AUTONOMOUS WHEELCHAIR

WITH DISTRIBUTED CONTROLS

3.1   Introduction

In this chapter, the details on the design and implementation of the SSVEP-based BCI wheelchair are discussed. Figure 3.1 shows the block diagram of the design. The BCI portion consists of an EEG acquisition hardware, signal processing with classification software, and SSVEP stimulus generation. The wheelchair portion consists of the navigation software interfacing with the sensors and motor controllers. Interactions between these components are shown in Figure 3.1. Each component shown in the block diagram will be discussed in detail in their respective sections later in this chapter.
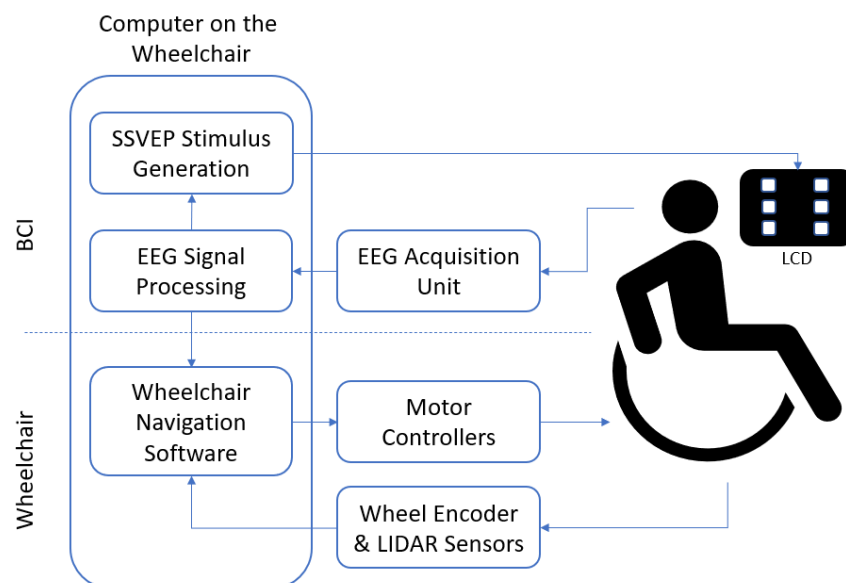
Figure 3.1   Block diagram for the design of SSVEP-based BCI autonomous wheelchair developed in this study.

A custom EEG acquisition unit was designed and developed for the wheelchair developed in this study. The details for the design of the hardware and firmware developed are described in Section 3.2 of this chapter. Section 3.3 covers the BCI software created for this study. The wheelchair used in this study is a modified version of a commercially available powered wheelchair. The details on the modification of the wheelchair are described in Section 3.4 of this chapter. The final section of this chapter will describe the methods implemented in the wheelchair navigation software.

3.2   EEG Acquisition Unit

A custom EEG acquisition unit for use with the wheelchair was developed. The requirement for the BCI acquisition unit for this study is to acquire EEG signals using the gold cup wet electrodes on a moving wheelchair. An analogue front-end that is capable of amplifying and applying signal conditioning on EEG signal between the range of 10μV to 100μV will be constructed. Besides, the EEG unit needs to be small, portable and can be powered through the USB port of a computer for its operation. A low-noise 24-bit Delta-Sigma analogue front-end, TI ADS1299 was used in this design for signal conditioning. ADS1299 have 8 differential analogue inputs for 8- channel EEG signal acquisition. This analogue front-end also has built-in bias drive amplifier and lead-off detection which are useful for EEG measurements. Programmable gains of 1, 2, 4, 6, 8, 12, or 24 can be selected through Serial Peripheral Interface (SPI) of the ADS1299. The differential amplifier of ADS1299 has a typical value of -120dB.The integrated programmable gain amplifiers (PGA) in ADS1299 coupled with the low noise characteristic and

high precision of the analogue front-end allow the acquisition of EEG signals with minimal extra components (Soundarapandian & Berarducci, 2010).

Figure 3.2 and Figure 3.3 show the schematic diagram of the EEG acquisition unit developed for this study. The detail bill of materials to build the circuit is listed in Appendix C. Each of the inputs is filtered by differential capacitors before the signals are fed into the differential inputs. A bias output from the ADS1299 is connected to the output pins for the bias electrode connection. The register of the ADS1299 can be configured to set the gain and the mode for each of the differential inputs. The ADS1299 is connected to a 16-bit microcontroller, PIC24FJ64GB8044 from Microchip. This microcontroller has all the required hardware such as internal oscillators, SPI peripheral and USB transceivers built-in. This reduces the need for external components to use the microcontrollers. Both the microcontroller and the analogue front-end are powered from a 3.3V source. A low drop out voltage regulator is used in the design to convert 5V from the USB to 3.3V to power both the microcontroller and the analogue front-end.
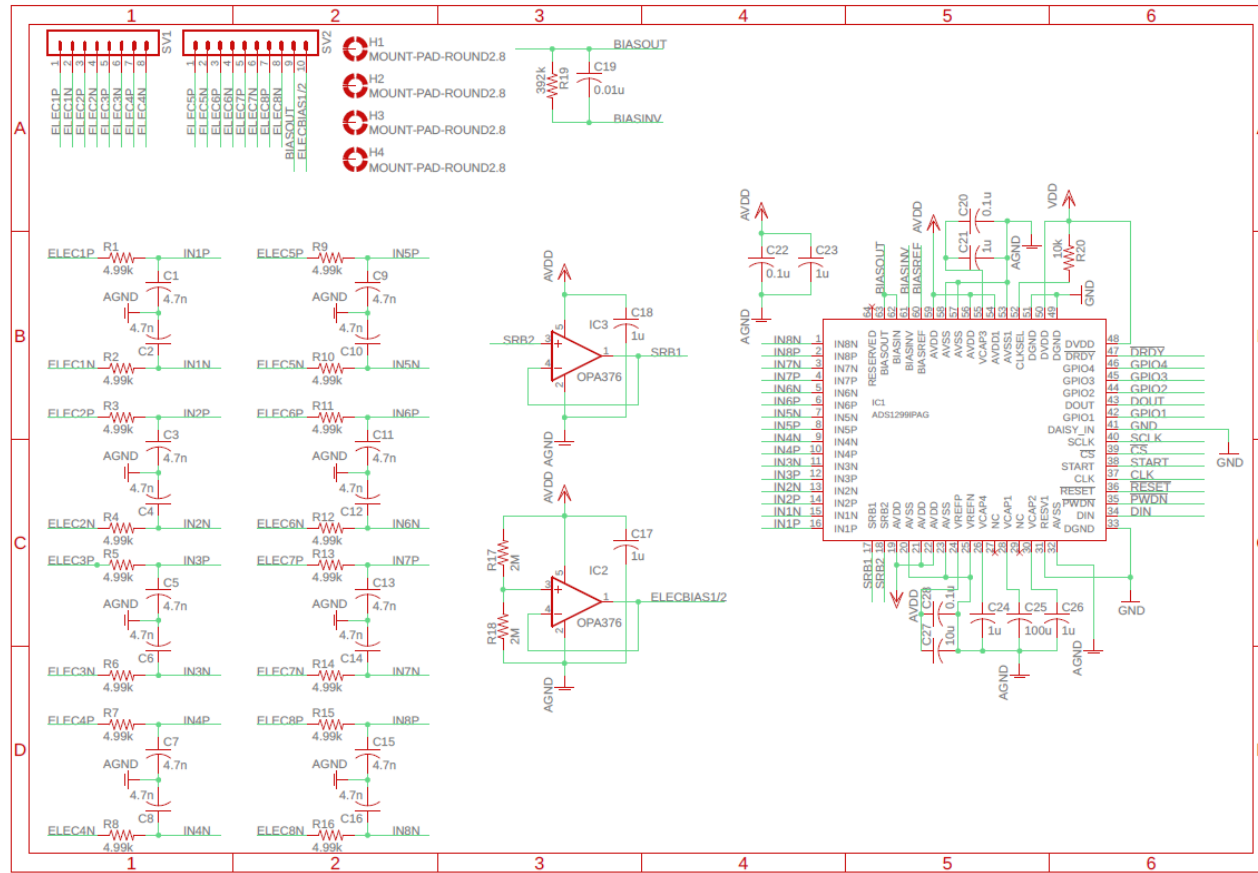
Figure 3.2   Schematic diagram of the EEG acquisition unit sheet 1 of 2. The ADS1299 is the PGA used in the design of the EEG Acquisition unit.

23
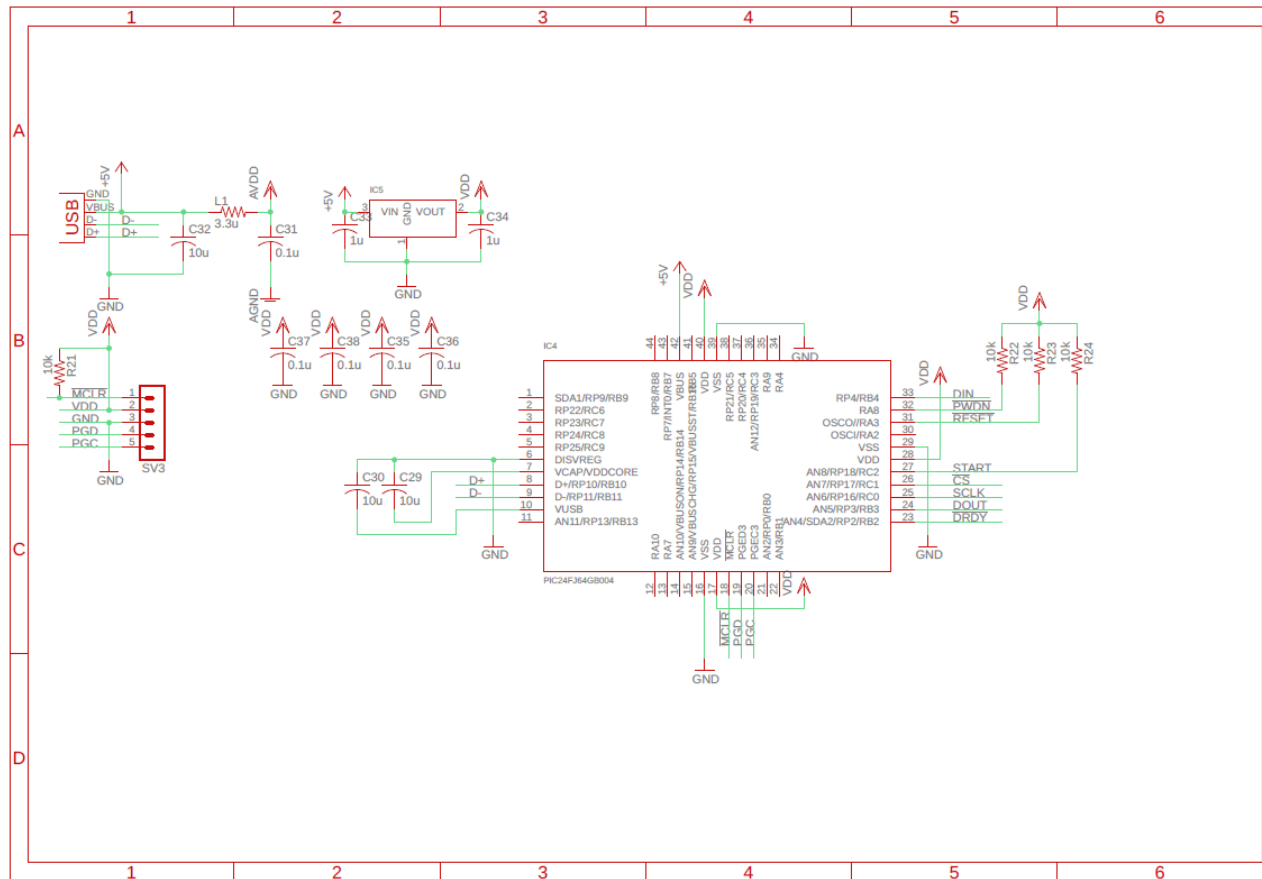
Figure 3.3   Schematic diagram of the EEG acquisition unit sheet 2 of 2. APIC24FJ64GB8044 is used as the USB microcontroller to transfer the data obtained from the ADS1299.
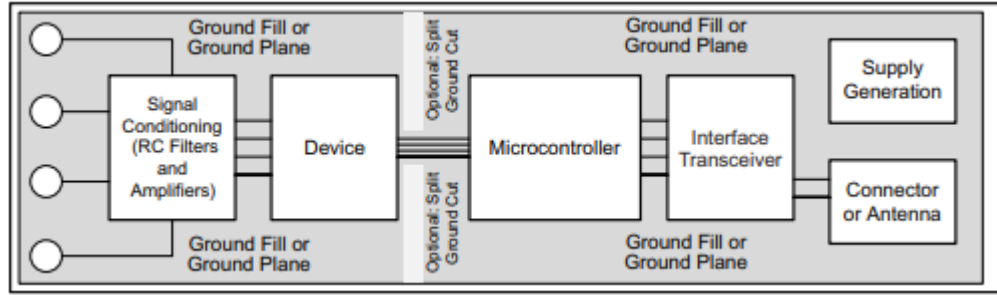
Figure 3.4   Best practice for the layout of components recommended by Texas Instruments for printed circuit board (PCB) using ADS1299 (Texas Instruments, 2017).

Based on the schematic diagrams, a PCB for the EEG acquisition unit was designed. Figure 3.4 shows the best practice when designing the layout of components to prevent noise from the high-frequency digital coupling back into the analogue signals. Ground fill or planes are recommended for void areas underneath the signal's routes. Splitting of ground planes between the analogue and digital ground planes is recommended. Figure 3.5 shows the design of a two-layer PCB for the EEG acquisition unit following the recommendations given by Texas Instruments. The board is separated into two portions by a split ground cut at 45° in the middle of the board. The digital portion of the circuitry which contains the microcontroller and USB is at the top right portion whereas the analogue circuitry is at the bottom left portion. The substrate use for the PCB fabrication is FR-4 with a thickness of 1.6mm and 1 oz copper. PCB surface finishing is conducted using electroless nickel immersion gold plating.
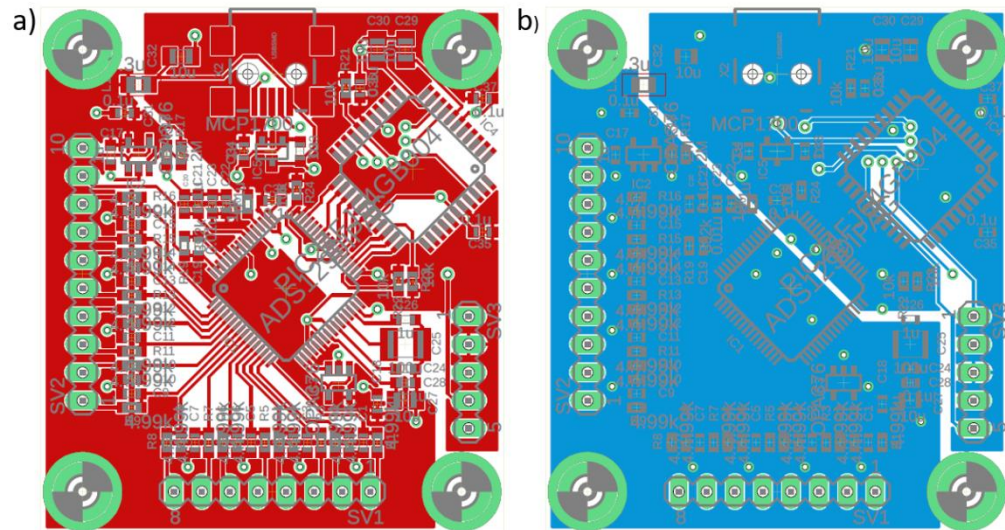
Figure 3.5   Two-layer PCB layout for the EEG acquisition unit. a) red layer is the copper traces for the top layer. b) blue layer is the copper traces for the bottom layer. Green colour traces in the figure pads for vias and components.

Digital signals from the ADS1299 analogue front-end are then fed to the microcontroller through SPI. Custom firmware was developed to interface with the ADS1299 through the USB. All the register of ADS1299 can be configured through the USB using the developed firmware. This allows the BCI software on the computer to access and configure all the features on the ADS1299 during operation. Settings such as the sampling rate, the number of channels sampled, and the PGA's gain can be adjusted through the firmware. The firmware is designed to send data according to the settings provided by the BCI software. Every EEG sample is 3 bytes in size. Depending on the number of channels and the sampling rate requested the packet size will change accordingly. The maximum sampling rate that the firmware can cater for is 250 samples per second for eight channels which translates to a data rate of 6kB per second. Pseudocode 3.1 shows the operation of the firmware created for the EEG acquisition unit.

```
Pseudocode 3.1: EEG Acquisition Firmware
01. Perform ADS1299 power-up sequence
02. Initialization of USB communication stack
03. Main loop:
04.     if new register setting is available
05.         update ADS1299 Register
06.     end
07.     if start acquisition
08.         while stop acquisition == false
09.             send raw adc data through USB
10.         end
11.     end
12. end
```

After power-on reset, the first routine the microcontroller performs is to initialize the ADS1299. There is a power-up sequence to power up the internal oscillator, the analogue and digital circuitries of the ADS1299. Once the power-up sequence is completed, the microcontroller will run an initialization routine for the USB communication stack. After the stack is initialized the software on the computer can communicate with the USB device. The firmware will wait for commands from the computer in the main loop. If the device receives new register settings for the ADS1299, the firmware will update the corresponding register in the ADS1299 accordingly. Start of acquisition can be triggered by the software in the computer through the USB. Leadoff detection is enabled during measurement to ensure that the EEG leads are connected properly during the acquisition. A notification will be sent to the computer if leadoff is detected. Raw ADC data will be stream to the computer once every sample is obtained from the ADS1299. No signal processing steps are conducted in the firmware. All further digital signal processing steps are conducted in the BCI software on the computer.

3.3   BCI Software

The BCI software developed in this study is responsible for the collection, processing and classification of EEG signals measured by the EEG acquisition unit. After a successful classification, the software will generate the corresponding control signals to drive the wheelchair. A user interface was also created to allow the users access to all the features developed to control the BCI wheelchair. Besides EEG-related tasks, the software is responsible for the generation of SSVEP stimulus. Figure 3.6 shows the block diagram and the sequence of the algorithm for the developed BCI software.

The software is responsible for the generation of visual stimulus. The visual stimuli used are white square patches flickering on black background. The stimuli are generated on an LCD screen. There will be a maximum of six stimuli present at any one time on the screen for selection. Each of the patches flickers at a different frequency, providing the subject with six different choices when looking at the stimuli. The frequencies at which the patches flickered are 7Hz, 11Hz, 12 Hz, 13 Hz, 14 Hz, and 15Hz. The frequency and location of the patches can be adjusted in the developed software.
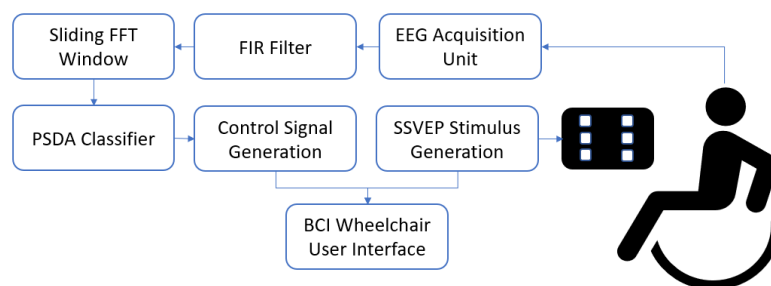
Figure 3.6   Block diagram of the developed BCI software. The software is responsible for the generation of stimulus and the classification of SSVEP.

Data obtained from the EEG acquisition unit are raw ADC values of the voltages detected on the electrode after amplification. The ADC values are converted into voltages before the filtering step. Equation (3.1) shows the calculation to obtain the voltage from the ADC value.

$$v = \left(\frac{X}{2^n} * V_{ref}\right) * \frac{1}{G} \tag{3.1}$$

where X is the ADC value, n is the bit of ADC, V_{ref} is the reference voltage and G is the gain of the PGA. The ADS1299 has a built-in 24-bit ADC and an internal reference of 4.5 volts. These 2 values are substituted in equation (3.1) for the calculation of voltage measured. The gain of the amplifier, G, can be adjusted in the software and will vary depending on the configuration used during measurement. The gain used throughout this study is 24. Using this equation, the value of the electric potential measured on the electrode can be obtained. The sampling rate of the EEG acquisition unit is set at 250Hz in this study. According to Nyquist theorem, the sampling frequency must at least be 2 times higher the maximum frequency in the measured signal (Ravanshad & Rezaee-Dehsorkh, 2020). The maximum frequency of interest measured in this study is 15Hz. The sampling rate of 250Hz is a suitable value for the EEG acquisition unit in this study.

After conversion, the sampled signal will passthrough a finite impulse response (FIR) filter. The FIR digital filter used in this study is a bandpass filter with a passband of 2Hz to 23Hz. The lower range of 2Hz is selected to remove low-frequency artefacts that may arise due to motion of the subject. The upper range of 23Hz is selected to remove powerline noise at 50Hz in Malaysia and

other high-frequency noise. The range of frequency for the measured EEG signal is in between the passband selected. FIR filter coefficients used by the software is created using filter designer from the signal processing toolbox of MATLAB. The filter is designed using the Equiripple method with the structure of Direct-Form FIR. The magnitude for the stopband is set at 80dB and 0.01dB is set for the passband. This results in a 1019 order FIR filter. Figure 3.7 shows the magnitude response of the designed filter. The large initial delay in the FIR filter is unavoidable in order to fulfil the passband, stopband, and slope requirements of the filter. The coefficients from the designer are exported for use in the BCI software.
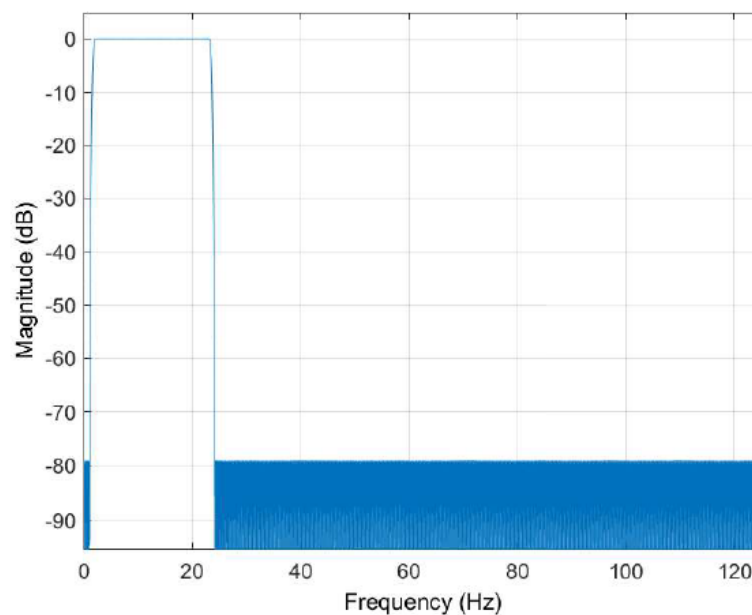
Figure 3.7   Magnitude response of the 1019 order Direct-Form FIR bandpass filter with a passband of 2Hz to 23Hz.

The step after filtering is to perform FFT on the filtered data. The power spectrum obtained from FFT is used as the feature for classification in this study. A sliding window is used to frame the data for FFT. The width of the window and step size can be adjusted in the software. Figure 3.8 shows an example of the sliding window used in the software developed. In this example, incoming EEG signals are segmented into a 2000ms sliding window with a step size of 250ms. FFT is conducted on each of the sliding window to obtain the power spectrum of the measured EEG signals.
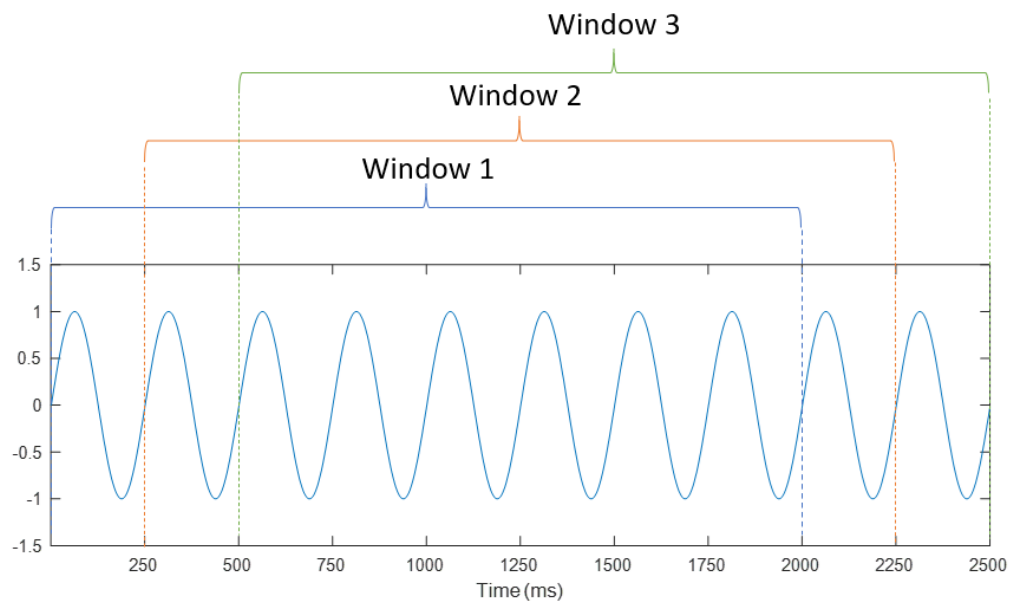
Figure 3.8   Sliding window over the measured signals. Window length used in this study is 2000ms. The step size of 250ms is used for the sliding window.

An adaptation of the PSDA classification algorithm is implemented for the classification. A successful classification of SSVEP is attained if the resultant FFT magnitude of the stimuli's fundamental frequency is higher than the threshold set for five consecutive windows. The threshold for detection was n times the mean value of the amplitude spectrum between 3Hz and 23Hz. The

multiplier, n for detection can be adjusted in the developed software. An event will be generated when a successful classification is generated. In this study, the threshold of n = 3 is used. This value is determined based on the data collected from the previous studies of my research team (Chin, 2017; Mah, 2017).

The BCI software was developed for both Windows and Ubuntu. In Windows, the software was developed as a .Net application written in the C# programming language. DirectX renderer is used to ensure the timing of patches can be controlled. For Ubuntu environment, the software was developed as a Robot Operating System (ROS) Node written in the C++ programming language. OpenGL was used in Ubuntu environment for the generation of the flickering.

3.4   Wheelchair Hardware

The wheelchair used in this study is a commercially available powered wheelchair Titan X23 from Drive DeVilbiss Healthcare. This wheelchair is a 24 V battery-operated wheelchair with a dimension of 952.5mm length, 596.9mm width, and 1104.9mm height. The maximum load that the wheelchair can carry is 136kg. The wheelchair is differentially driven by 2 motors each with a power of 270W. The wheelchair was modified to convert it to a wheelchair capable of autonomous function. Sensors were added and the driver for the motor was changed so that the wheelchair can be driven autonomously. Extra mechanical structures were also added to cater for the mounting of sensors used for the wheelchair.

Sensors added to the wheelchair include wheel encoders, ultrasonic range sensors, an inertial measurement unit (IMU), and laser range finders. The wheel shaft was modified to enable the installation of wheel encoders on both the left and right drive wheels. Two incremental type shaft encoders with a resolution of 500 pulses per revolution with two phase output were installed in the wheelchair. Each of them was connected to the wheel through a pulley system. The pulley mounted on the encoder is connected to the pulley mounted on the wheel by a synchronous belt. The diameter of the pulley mounted to the wheel shaft is 48mm with 30 teeth and the pulley mounted to the encoder is 15.66mm with 10 teeth. The wheel diameter of the wheelchair is 257. 8mm.From these values, the distance travelled by each of the wheel can be calculated from the encoder readings. Equation 3.2 shows the calculation for the distance per pulse,

$$distance\ per\ pulse = \frac{\mathrm{d}_{wheel}}{3*4*\mathrm{n}} = 0.043mm \qquad (3.2)$$

where d_{wheel} is the diameter of the wheel, 3 is the ratio of the pulley, 4 is the multiplier for encoder running in quadrature mode and n is the number of pulses per revolution for the encoder. From the calculations, the distance per pulse detected is 0. 043mm.This value was used as one of the inputs for the odometry calculation of the wheelchair.

Ranged sensors such as ultrasonic and laser range finders were installed on the wheelchair to detect the surrounding environment. A tray was added in front of the seat for the mounting of front-facing sensors. This tray was also used to place the computer and the EEG acquisition unit. Ultrasonic sensors

from MaxBotix operating at 42KHz with a detection range of 0.03m to 5m was mounted at the front of the wheelchair. Besides the ultrasonic sensors, a laser range finder, URG-04LX-UG01 from Hokuyo with a maximum detection distance of 5.6m over 240° angle with an angular resolution of 0.325° was also fitted at the front tray. Both sensors provide information about the surrounding to the navigation software.

A navigation laser range finder, NAV350 from Sick was also added to the wheelchair to allow the wheelchair to see further. The navigation laser range finder has a maximum scanning range of 250m with the capabilities to detect specific reflectors landmark within a range of 70m. This laser range finder can obtain readings over 360° angle with an angular resolution of 0.1°. Besides this, the navigation laser range finder also has a position function where the navigation laser range finder can calculate it's position relative to the landmarks detected given a map and odometry values. However, due to the 360° angle operation range of the navigation laser range finder, it was mounted above the head of the passenger on the wheelchair. The wheelchair was modified with extra supporting structures at the back so that the navigation laser range finder can be mounted. The support was designed so that the laser operating height was set at 1.8m. This height was selected so that the bottom of the navigation laser range finder was 0.5m above the headrest of the wheelchair. This will ensure that the wheelchair and the subject sitting on the wheelchair will not block the line of sight of the navigation laser range finder. Figure 3.9 shows the modification on the wheelchair to accommodate the wheel encoders, ultrasonic sensors, obstacle, and navigation laser range finders.
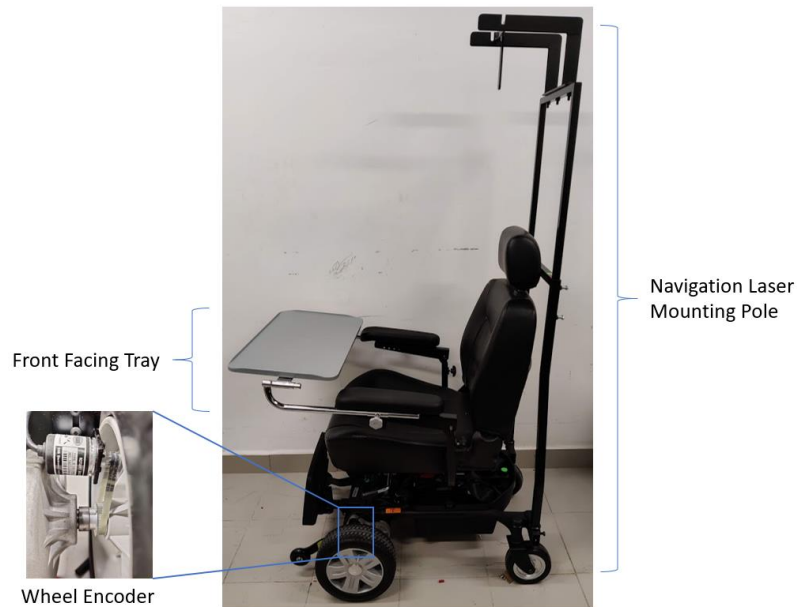
Figure 3.9   The modification conducted on the wheelchair for the mounting of sensors. Extra structures are added to the wheelchair so that the navigation laser pole can be added at the back of the wheelchair. The front-facing tray is mounted to the armrest of the wheelchair. Pulleys were added to both wheels as the interface with the wheel encoders through the belts.

The obstacle laser range finder was connected to the computer directly through the USB interface while the navigation laser range finder was connected to the Ethernet interface of the computer. A wheelchair control board was designed to interface with other sensors and to control the wheelchair motor. Other sensors such as the ultrasonic range sensor and the wheel encoders were connected to the wheelchair control board. Figure 3.10 shows the schematic diagram of the wheelchair control board. The control board was designed to be able to interface with two wheel encoders and a maximum of five ultrasonic sensors. The board and sensors connected were powered through the USB port.
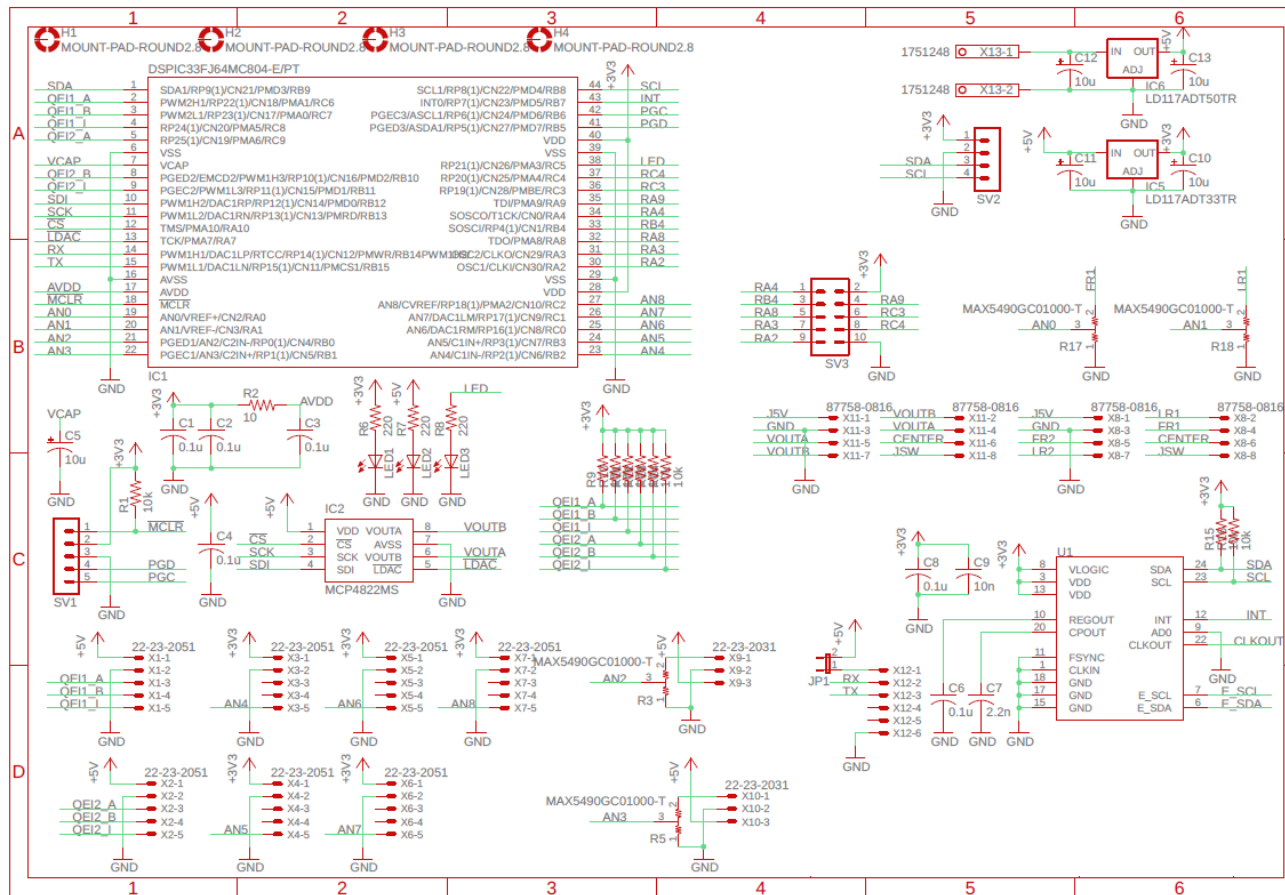
Figure 3.10   Schematic diagram of the wheelchair control board.

A microcontroller designed for motor control from Microchip, DSPIC33FJ64MC804 was used as the controller for the wheelchair control board. A 9 axis IMU, MPU-9250 was incorporated into the wheelchair control board as well. The IMU consists of a 3-axis accelerometer, a 3-axis gyroscope and a 3-axis magnetometer. The I2C communication protocol was used for the communication between the IMU and the microcontroller. A digital to analogue converter was used to control the motor driver of the wheelchair. The motor driver used for the wheelchair is a 60A dual-channel DC Motor Driver, MDDS60 from Cytron. The analogue operating mode of the driver is used for driving the motors of the wheelchair. A USB to UART convertor was used to interface the wheelchair controller board and the wheelchair software in the computer. Figure 3.11 shows the PCB designed based on the schematic diagram in Figure 3.9.
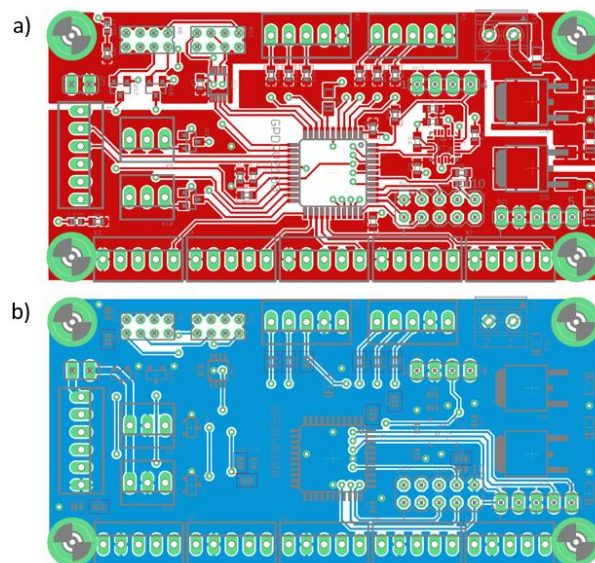
Figure 3.11   2-layer PCB layout for the wheelchair control board. a) red layer is the copper traces for the top layer. b) blue layer is the copper traces for the bottom layer. Green colour in the figure traces pads for vias and components.

```
Pseudocode 3.2: Wheelchair Controller Firmware
01. Perform IMU9250 power-up sequence
02. Setup UART and Digital to Analogue Convertor
03. For every 50ms:
04.     Sample IMU sensors value
05.     Update control value obtained through UART
06.     Calculate Odometry values using indirect
        feedback Kalman filter.
07.     Send Odometry and IMU values through UART
08. end
```

Pseudocode 3.2 shows the routine conducted by the firmware every 50ms. The control speed for the wheelchair was determined by the navigation software in the computer. For safety purposes, if the wheelchair controller firmware does not receive any control value from the computer within the 50ms timeframe, the firmware will execute an emergency stop. This is to prevent any unwanted incidents when there is an accidental disconnection between the computer and the wheelchair control card. For odometry calculations, the firmware implementation for the calculation of odometry through the fusion of encoders and gyroscope value using indirect feedback Kalman filter by Soh is used (Soh, 2018). Once the firmware obtained the IMU values from the sensor and odometry values from the calculation, the data will be sent to the computer through the UART interface.

3.5   Wheelchair Navigation Software

The software designed for the wheelchair must be able to integrate all the sensors provided to perform the navigation task and to conduct navigation decisions by interpreting the EEG software output. This is needed to ensure that

the wheelchair can navigate autonomously. This is important to achieve the distributed control system needed to control the wheelchair autonomously using SSVEP BCI. To achieve autonomous navigation, the wheelchair navigation software needs to interface with all the sensors that were installed. The developed software interfaces with the sensors and controller through the USB and Ethernet interface. Figure 3.12 shows the block diagram for the software created.
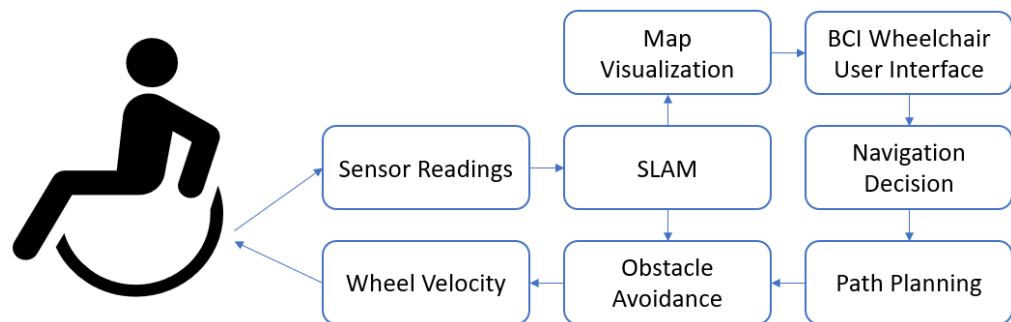
Figure 3.12   Block diagram of the wheelchair navigation software. The software is responsible for, SLAM, path planning and obstacle avoidance.

Two modes of operation were developed for the wheelchair. The first is the destination mode where the user only selects a destination. The wheelchair will be moving to the destination without further input needed from the user. For this mode, the wheelchair can only operate in a known environment where the map of the surrounding is available. The second mode of operation developed for the wheelchair is the directional mode. In this mode, the user will be selecting a direction of travel for the wheelchair, the wheelchair will move in the direction selected while planning the path with a custom exploration algorithm. For this mode, the wheelchair can be operated in a known or unknown environment. SLAM will be conducted by the wheelchair in this mode.

The map generated in the directional mode can later be used in the destination mode.

SLAM in the directional mode is implemented using Cartographer SLAM (Hess, et al., 2016). Cartographer is a system that can conduct real-time SLAM in 2D and 3D environments. Cartographer SLAM has two main subsystems, the local SLAM and Global SLAM subsystems. The local SLAM is tasked with generating good submap from the input sensors. The global SLAM takes in the submap generated by the local SLAM and performs scan-matching for loop closure joining the submaps to generate a map of the surrounding. Laser range finders mounted on the wheelchair are used as the input sensor for SLAM. Fixed cell maps generated from SLAM can be used for both directional and destination mode.

A custom exploration algorithm for the wheelchair was developed for the directional operation mode. The custom exploration algorithm is a laser-based frontier detection and waypoint generation. Pseudocode 3.3 shows the steps taken for the generation of waypoints for navigation in directional mode.

```
Pseudocode 3.3: Exploration Algorithm
01. For every Laser Scan:
02.     Obtain the robot location from SLAM
03.     Identify new region from laser scan
04.     Calculate centroid of traversable region
05.     Publish centroid of marker as viable
        waypoints for motion
06.     Update waypoints status
06. End
```

A frontier is defined as a segment that separates the explored and the unknown regions for a robot (Yamauchi, 1997). A frontier can be detected by overlapping the scan region from laser scans and the map generated by SLAM. Figure 3.13 shows an example of a frontier in the directional operation mode. The laser scan result will determine whether the frontier is traversable or not. If no obstacle is detected by the obstacle sensors, the frontier region will be marked as traversable by the algorithm.
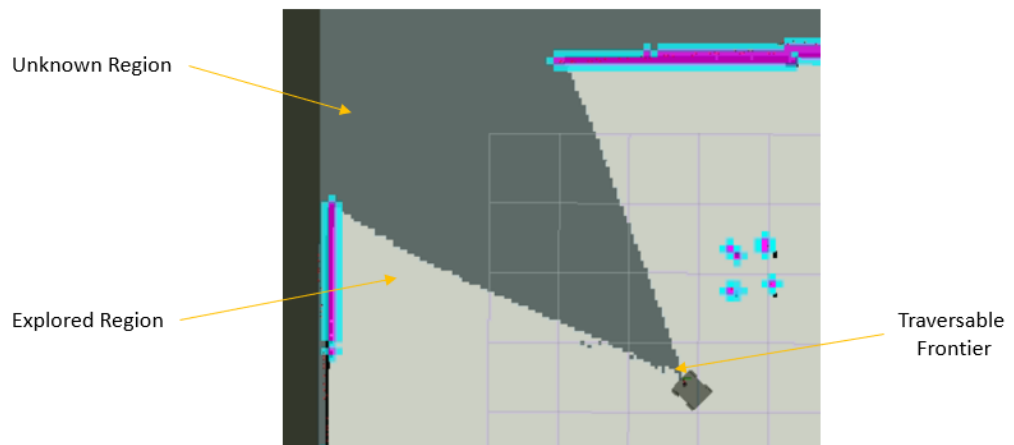
Figure 3.13   The explored region is indicated by the light grey colour in the map generated. The unknown region of the map is coloured dark grey. The intersection between the unknown region and the explored region is the frontier.
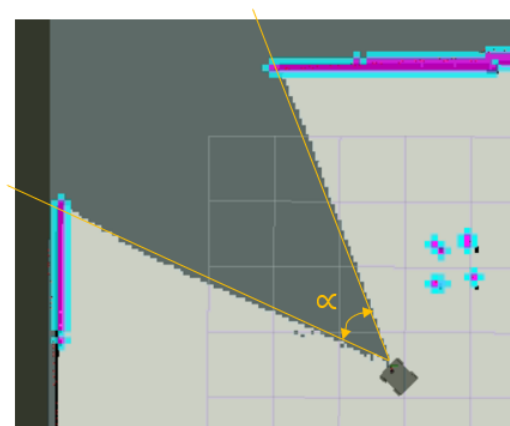
Figure 3.14   An example of a traversable unknown region, α is the angle between the start and end of the traversable region as detected by the laser range finder.

41

Waypoints are generated from the centroid of newly detected traversable regions. A traversable region is defined as a continuous region between two laser scans where the underlying region is unknown. Figure 3.14 shows an example of an unknown traversable region. α is the angle between the start and the end of the traversable region. The angle α of a region needs to be larger than 10°. This is to ensure that the wheelchair can move past the frontier region detected. If the angle α is larger than 45°, a new traversable region is created. This is to ensure that waypoints in multiple directions were generated by the exploration algorithm when the wheelchair is in wide open space. Equation 3.3 shows how the centroid distance of the region is calculated.

$$d_{centroid} = \frac{2 \sin(\alpha) * scan_{max}}{3\alpha} \tag{3.3}$$

where α is the angle between the start and end of the traversable region and $scan_{max}$ is the maximum scan distance of the laser range finder used for the exploration algorithm.
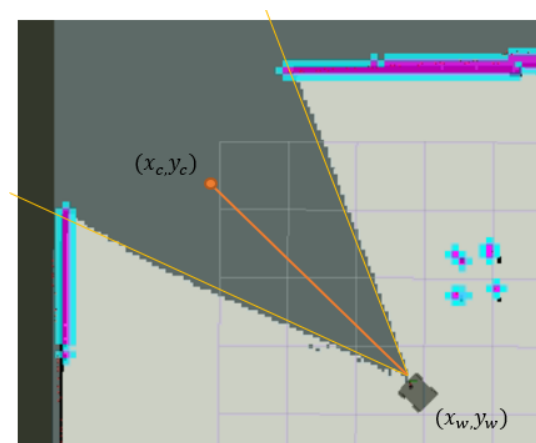
Figure 3.15   Coordinate of centroid and the coordinate of the wheelchair referenced to the generated map.

The centroid is located at $\alpha/2$ from the start of the traversable at a

42

distance of $d_{centroid}$ from the current position of the wheelchair. Figure 3.15 shows an example of a centroid obtained from using Equation 3.3. The next step for the exploration algorithm is to generate the coordinates of the waypoints to the map frame from $d_{centroid}$ and the angle. Equation 3.4 shows the calculation of the waypoint coordinates referenced to the map frame generated by SLAM,

$$\begin{bmatrix} x_c \\ y_c \end{bmatrix} = \begin{bmatrix} x_w \\ y_w \end{bmatrix} + \begin{bmatrix} \cos\left(\theta_s + \frac{\propto}{2}\right) \\ \sin\left(\theta_s + \frac{\propto}{2}\right) \end{bmatrix} * d_{centroid} \qquad (3.4)$$

where (x_c, y_c) is the coordinate of the centroid, (x_w, y_w) is the coordinate of the wheelchair, θ_s angle for the start of the traversable region referenced to the map frame, $\propto/2$ is the angle of the centroid and $d_{centroid}$ is the distance obtained from equation 3.3 .Once the coordinate of the centroid referenced to the map frame is generated, a conditional check is performed to ensure that the Euler distance between the newly generated waypoint is at least 0.3 times of $scan_{max}$ for the new waypoint to be registered. At the end of every laser range finder scan cycle, all waypoints will be checked and updated. If any of the waypoints on the explored region of the map, the waypoints will be marked as explored else the status will be kept as unexplored.

The directional mode uses the waypoints generated by the exploration algorithm for navigation. In this mode, four quadrants (front, back, left and right) will be presented to the user. Once the user of the wheelchair made a selection, the wheelchair will move towards the nearest waypoint detected in the quadrant selected by the user. For directional mode, the wheelchair will continue to move until there is no new waypoint generated in the direction of

travel selected by the user. The envelope of travel for the quadrant depends on the location of the wheelchair when the directional travel is initiated. Figure 3.16 shows an example of the four quadrants available for selection in the directional mode. In the directional mode, the user can trigger and save the current coordinate of the wheelchair for use in the destination mode.
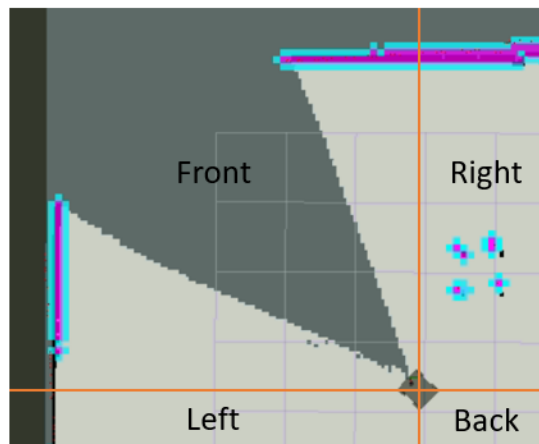
Figure 3.16   The 4 quadrants of travel available for the wheelchair in directional mode.

For the destination mode, the wheelchair will be using a predefined map for navigation. The predefined map can be the map generated by SLAM in the directional mode or a pre-programmed map in the software. In this mode, the wheelchair can only move within the explored region up to the boundary as defined by the map. Any goals given to the wheelchair in the unknown region will not trigger any movements. Adaptive Monte Carlo localization (AMCL) was applied to localize the wheelchair in the map selected. Monte Carlo localization is a set of probabilistic algorithms which utilizes particle filter to determine the position information of a robot on a map (Thrun, et al., 2001).Adaptation of the sample size during the estimation process for MCL using KLD-resampling increases the efficiency of the particle filter (Fox, 2003).

AMCL will generate an estimated position for the wheelchair reference to the map frame. Path planning and navigation can be conducted by the wheelchair in destination mode when the wheelchair knows the current position.

Both destination and directional modes use the same navigation stack to control the motion of the wheelchair. The navigation stack is separated into global navigation and local navigation. The global navigation will seek out the path needed for the travel to a given destination. A* path planning algorithm is used to get the global path for the robot to travel to. A* path planning aims to find a path to the given goal with the shortest distance from the current position (Ferguson, et al., 2005). The algorithm achieves this by doing an iterative search measuring the Manhattan distance to the goal at every step and creating the shortest path incrementally.

Once a path is found, the wheelchair can navigate to the destination following the path. The local path planner is responsible for the control of the local trajectory of the wheelchair in the local frame. The local frame is a 4m x 4m square region with the wheelchair in the middle of the region. Time Elastic Band (TEB) path planner is implemented as the local path planner. TEB can compute the optimal trajectory by solving a sparse scalarized optimization problem (Rosmann, et al., 2013). The weights for the optimization problem can be changed to specify the behaviour of the local planner on the motion of the wheelchair. The local planner for the wheelchair is set to run the optimization step every 50ms. Any obstacle newly detected by the ultrasonic or the laser range finders is added to the local costmap used for TEB path planning. The local planner will avoid any obstacle while following the global path to the

destination selected. Control signals for the wheelchair will be generated by the navigation stack and passed to the wheelchair controller through the USB to serial converter.
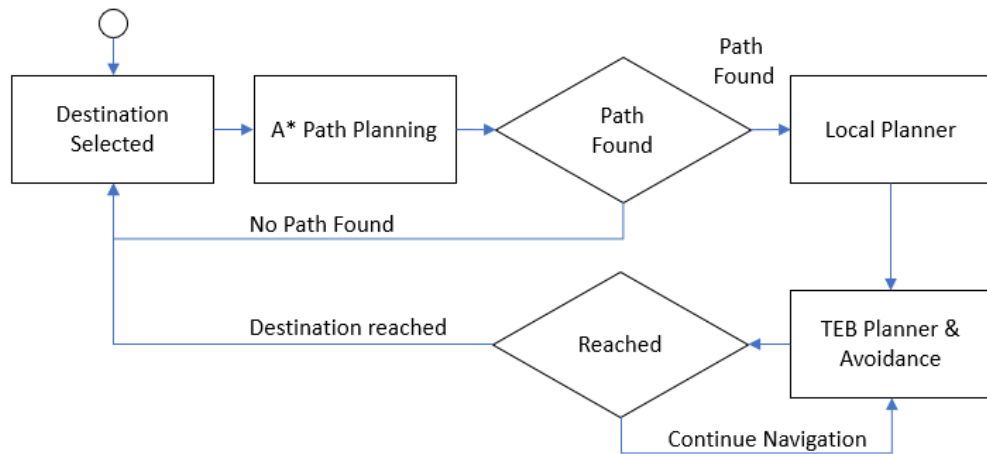
Figure 3.17   Flowchart of the navigation software for both the destination and the directional modes.

In the event where there is no viable path within the local space, the wheelchair will attempt to search for a new global path. If both the local and global planner failed to find a viable path, the wheelchair will stop and inform the user to select a new direction or destination. Figure 3.17 shows a flowchart summary for the navigation software.

3.6   SSVEP BCI Autonomous Wheelchair with Distributed Controls

The SSVEP BCI autonomous wheelchair with distributed controls is achieved by combining the EEG acquisition unit, EEG software, wheelchair controllers, sensors and the wheelchair software as described in section 3.2 to 3.4. The main objective of this study is to create a system to minimize inputs from the user to get to an intended destination. To achieve this the multiple decision-making processes of navigating the wheelchair needs to be separated from the BCI. The SSVEP based BCI selection can be considered as a discreet selection where there are 2 states detected or not detected for each of the stimulus frequency. The number of distinct actions that can be triggered by the SSVEP BCI depends on the number of stimuli available on-screen at any one time. In this study, the number of stimulus on screen is limited to a maximum of 6 at any one time resulting in a maximum of 6 different selections available to the user of the BCI wheelchair.
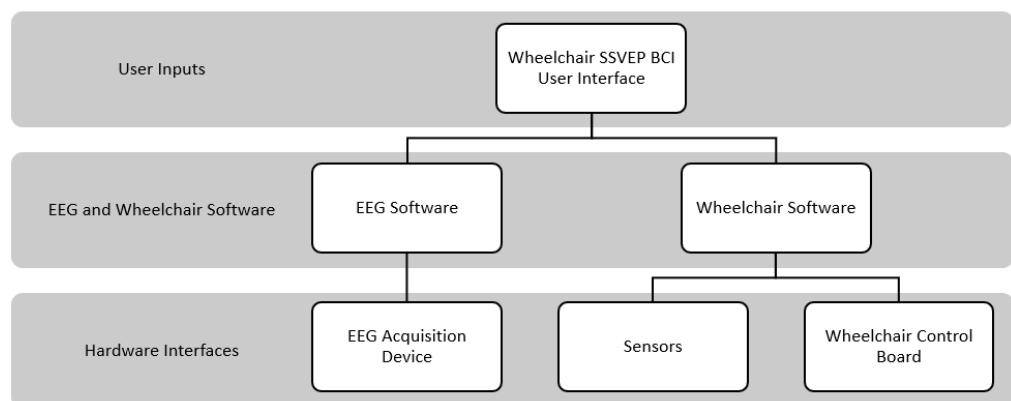
Figure 3.18   Interface between the user interface, software, and hardware for the SSVEP BCI Autonomous Wheelchair.

Figure 3.18 shows the interface between each of the components of the wheelchair. Inputs from the user will determine the operation mode of the

47

wheelchair. The user does not control the wheelchair directly using the SSVEP BCI. The user only gives high-level commands through the BCI to control the wheelchair. In directional mode, the direction of travel is passed to the wheelchair software. In the destination node, the destination of travel is passed to the wheelchair software. The task of controlling the motion of the wheelchair is distributed to the software and firmware level from the user. As described in section 3.4, the wheelchair software will conduct path planning and obstacle avoidance to navigate the wheelchair to a destination automatically. While the wheelchair is moving, the user can trigger the wheelchair to stop using the BCI user interface. Task such as obstacle avoidance that is not easily achieved with direct BCI driven wheelchair can be done autonomously by the wheelchair control software. The capability of avoiding an obstacle as well as a safe controlled emergency stop when a moving obstacle suddenly appears in the path of the wheelchair are very important features for a wheelchair operated using BCI. These features are integrated into the wheelchair path planner to ensure the safety of user with severe mobility impairment when using the wheelchair. In the firmware and hardware level, the system is designed so that the wheelchair will also perform a safe controlled emergency stop when there is any disconnection between the software level and the hardware interfaces. Issues such as loss of sensors reading and the disconnection with the EEG interface or the wheelchair controller will put the wheelchair into the emergency stop mode. The safety of the user is one of the key factors that is considered when the wheelchair is designed.

CHAPTER 4

RESULTS AND DISCUSSION

4.1   Introduction

This chapter focuses on the results and discussion from this study. Section 4.2 focuses on the EEG obtained using the acquisition system and the accuracy of the BCI software. The result for the destination-based control of autonomous wheelchair using SSVEP-based BCI is discussed in Section 4.3. Section 4.4 details the functions and experimental results for the wheelchair software. The last part of this chapter covers the comparison between distributed control scheme against SSVEP-based BCI to control the wheelchair directly.

4.2   EEG Acquisition System and BCI Software

The EEG acquisition unit described in Section 3.2 was fabricated and used as the acquisition unit for the wheelchair in this study. Figure 4.1 shows the fabricated EEG module housed in an aluminium case. In this study, EEG was obtained from the gold-plated reusable EEG cup electrode placed on the Oz position. The mastoid positions, M1 and M2 served as the reference and the ground for the measurements. For all measurements conducted in this study, each location where the electrode was placed was prepped with a mild abrasive (NuPrep skin prep gel). The cup electrode was filled with Ten20 electrode paste and covered with a piece of cotton and secured with medical tape to ensure that the electrode was in proper contact during measurements. A 2.2GHz Intel Core I5 laptop with 4GB RAM was used to run the developed BCI software.

Figure 4.1   Fabricated EEG acquisition unit housed in an aluminium case with 3 terminals for signal, ground and reference.
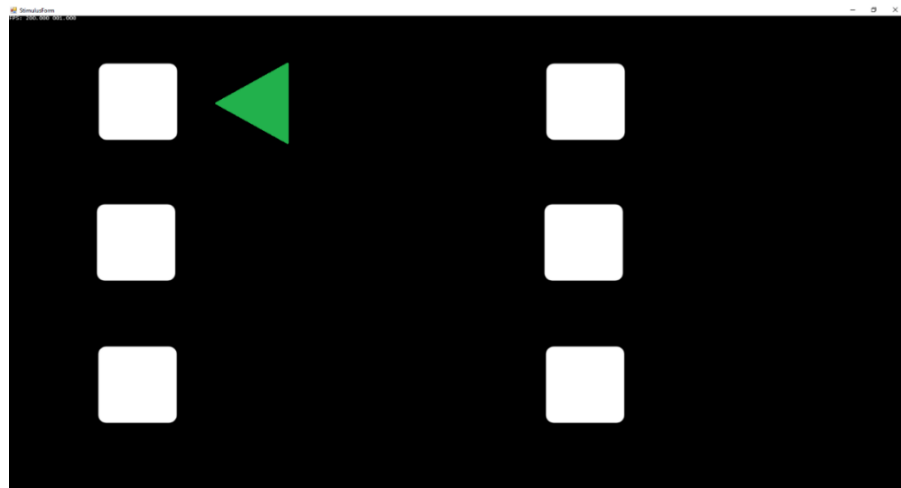
Figure 4.2   Selection GUI for the accuracy test. A green triangle arrow indicates the stimulus targeted for selection.

A study was conducted to test the accuracy of the developed EEG acquisition and BCI software. In the study, each subject was required to undergo three accuracy trials. The subject was required to complete a 12-selection task by looking at the stimulus on the selection GUI as shown in Figure 4.2 in each of the accuracy trial. Each selection task consists of a rest period of 5s where the screen was fully black and another 5s of selection period where the screen

contained the stimulus. A target location was chosen randomly out of the 6

frequencies for selection. A triangle green arrow would appear beside the

stimulus 1s before the stimulus started to flicker. The arrow only indicates the

target for selection and will not affect the classification result.
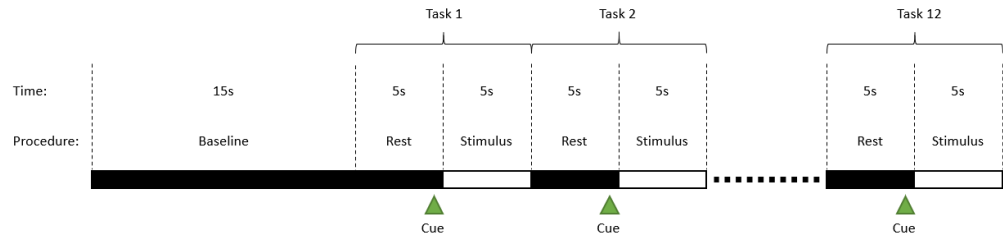
Figure 4.3   Experimental steps taken for the accuracy trial. Black colour in
the bar represents the time when the screen is black without
stimulus while white represents the time when the stimuli were
flickering. The green triangle below the bar indicates the time
when the cue is given by the software. A 15s baseline is added in
front of the study to record EEG baseline of the subject before
the starts of the trial. The selection task where the subject is
required to select were repeated 12 times for each trial.

Figure 4.3 shows the experimental steps conducted for the accuracy trial.

Each frequency would be chosen twice within a single duration of the accuracy

trial. The frequencies used for the accuracy test were 7Hz, 11Hz, 12Hz, 13Hz,

14Hz, and 15Hz. Each of the participants in this study was required to repeat

the accuracy trial 3 times. EEG signal recorded when the stimuli were on would

be passed to the classifier as described in Section 3.3 for classification. The

result for classification was recorded and saved for review after the accuracy

trials. The classification accuracy was calculated using Equation 4.1,

$$Accuracy = \frac{TP+TN}{TP+TN+FP+FN} * 100\% \qquad (4.1)$$

where TP represents true positive, FP represents false positive, TN represents

true negative, and FN represents false negative. TP is when the classification result of SSVEP matches the stimulus frequency of the flickering patch shown by the green triangle arrow for a given task. For the accuracy trials, TN is always equal to zero because no selection can be done during the rest period. FP is when the classified SSVEP indicates a different frequency compared to the one that is pointed out by the green triangle arrow. FN is counted when there is no successful classification during the 10s period for a task. For a given accuracy trial the denominator of the equation can be simplified to 12 as the sum of TP, FP and FN will be 12 given the number of tasks for one accuracy trial. This will simplify equation 4.1 to the equation (4.2)

$$Accuracy = \frac{TP}{12} * 100\% \qquad (4.2)$$

A total of five subjects were recruited for the study to test the accuracy of the developed EEG acquisition and BCI software. All the participants of this test had previous experience of using a BCI system. Participants of this study were aged between 23 and 28 when this study was conducted. Instructions and training for the accuracy trials were given to the subjects before the commencement of this study. All three trials were conducted on the same day and the result for the study is shown in Table 4.1.

Table 4.1:   Accuracy results obtained by the 5 subjects for the 3 trials.

	Trial 1	Trial 2	Trial 3	Average
Subject 1	100.00%	91.67%	100.00%	97.22%
Subject 2	91.67%	83.33%	91.67%	88.89%
Subject 3	66.67%	91.67%	83.33%	80.56%
Subject 4	83.33%	75.00%	100.00%	86.11%
Subject 5	91.67%	83.33%	83.33%	86.11%

The BCI system that was implemented for this study achieved an overall accuracy of 87.78%. Table 4.2 listed the number of false positives and false negatives recorded over the 3 trials. FP occurred when the classified frequency was different compared to the frequency of the stimulus pointed by the green arrow. This might be due to the subject looking at stimulus a frequency other than the one that was pointed out by the green arrow during the trial. FN might occur if the resultant FFT magnitude of the stimuli' fundamental frequency was not higher than the threshold set for 5 consecutive windows.

Table 4.2   Number of false positives and false negatives from the accuracy study

	False Positive	False Negative
Subject 1	1	0
Subject 2	2	2
Subject 3	3	4
Subject 4	1	2
Subject 5	1	4
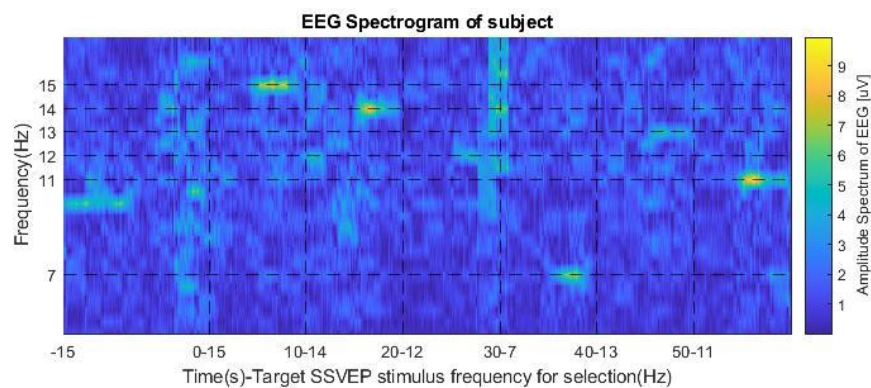
Figure 4.4   EEG Spectrogram of a subject undergoing an SSVEP accuracy trial. The baseline and 6 tasks are shown in the EEG spectrogram. The label on the x-axis indicates the start time of the first task and the frequency of stimulus pointed by the green arrow.

Figure 4.4 shows an example of the EEG spectrogram of a subject during

the first 6 tasks within the accuracy trial. The spectrogram shows the SSVEP measured in the EEG signal of the subject. During the period of stimulation, the resultant FFT magnitude of the stimuli' fundamental frequency indicated by yellow colour is higher compare to the magnitude of other frequencies.

The accuracy study showed that the developed EEG unit can classify SSVEP signals when the subject was looking at the stimulus. In this study, the threshold for the BCI system was fixed at three times the average of the FFT window. If the threshold is to be customized individually for each of the subject, the number of false negative would be reduced. The setup similar to the accuracy study would be used as the BCI input for the control of the autonomous wheelchair. Besides the current study, the BCI system developed was also used for the study to develop an SSVEP based communication interface (Mah, 2017; Mah, et al., 2019) and study of the effect of age on SSVEP signals (Chin, 2017).

The EEG acquisition device was designed to be safely operated using a battery-powered laptop. Any connections to the main power supply (240V, 50Hz) are not allowed during the EEG acquisition. This is to ensure that there is no pathway of current flow from the subject to any AC power source. The leakage current for the electrodes is rated at 110pA (Texas Instruments, 2017). This leakage current is safe for the users of the EEG acquisition unit.

4.3 Preliminary Study on Destination based Control of an Autonomous Wheelchair

A preliminary study was conducted to study the feasibility of controlling

an autonomous wheelchair through the selection of destination using SSVEP-based BCI. Figure 4.5 shows the block diagram of the SSVEP-based BCI autonomous wheelchair used in this study. The setup of the wheelchair used in the study is shown in Figure 4.6.The wheelchair software was configured to work with a preconfigured map for navigation. The built-in capabilities of the NAV-350 navigation laser range finder for localization was used to localize the wheelchair in the given map. Ultrasonic sensors were mounted in the front of the wheelchair for obstacle avoidance.
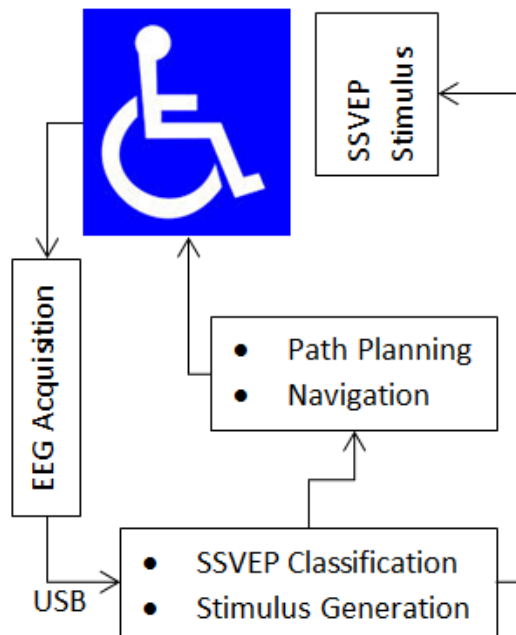
Figure 4.5   System block diagram for the SSVEP BCI wheelchair in the preliminary study.

Figure 4.6 Prototype autonomous wheelchair with PC, BCI acquisition unit, NAV350 navigation laser range finder and ultrasonic sensors

Figure 4.7 shows the placement of the stimulus on the computer screen. Each of the stimulus represents a pre-set location the wheelchair can move to. Once a destination is selected, the navigation software will plan the shortest path to the destination using A* algorithm. The wheelchair will navigate autonomously from the current location to the selected destination.

Figure 4.7 Interface for destination selection. There are four destinations (A, B, C, D) to choose from in the BCI GUI. The return selection is to close the application.
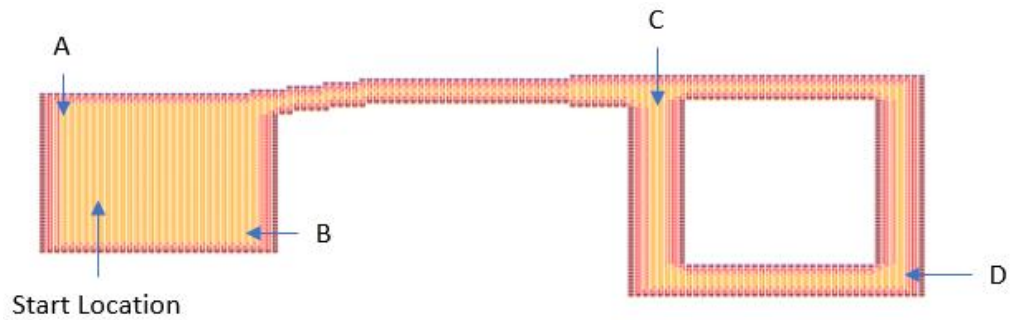
Figure 4.8   Preconstructed map with the 4 locations corresponding to the selections marked. Yellow colour in the map indicates areas which the wheelchair can navigate, while red indicates areas where it cannot.

The trial for the wheelchair was conducted in a lab located at Universiti Tunku Abdul Rahman. Figure 4.8 shows the pre-constructed map used by the wheelchair for navigation. The yellow colour on the map indicates the area where the wheelchair can move through. For this trial, four locations indicated by A, B, C and D were set at the fixed location when the map was constructed. The same subjects that had gone through the accuracy study described in Section 4.2 were recruited to undergo the preliminary study for the destination-based control of the wheelchair. In this study, the subjects were required to complete a series of selections to move the wheelchair around the preconstructed map. Figure 4.8   shows the start location and the four destinations that the subjects were required to select for the trial. The subjects were required to select and move the wheelchair in the following sequence, Start, D, C, B, A. Figure 4.9 shows an example of the path generated once the subject selected D as the destination for the wheelchair. From the trials, all subject successfully completed the tasks of moving the wheelchair to the four destinations.
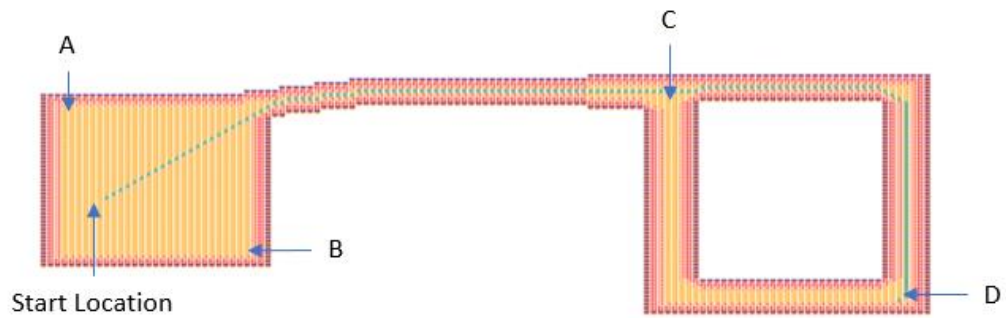
Figure 4.9   Path taken by the wheelchair after a subject selected to move to location D using BCI SSVEP from the start location.

This study showed the prospect of using an autonomous wheelchair where the SSVEP BCI system was only used for destination selection. On receiving the destination information, the distributed wheelchair controller successfully navigated the wheelchair to the selected destination avoiding obstacles on the way (Ng, et al., 2014). However, a destination only system is not that useful in the real-world setting. There is a possibility that the location the subject wanted to go to is not part of the pre-programmed destination. This is a drawback of using a destination only system. Therefore, a directional based system as described in Section 3.4 is added to the wheelchair software.

4.4   SSVEP BCI Autonomous Wheelchair with Distributed Controls

Robot Operating System (ROS) is used to implement the wheelchair software for the full system which incorporates the directional and destination systems. ROS is an open-source robotics middleware for the control of a robotic system with a well-established ecosystem for tools related to autonomous robots. In ROS, nodes are the execution blocks that are responsible for the execution of algorithms. Nodes can be combined into a graph and communicate with each other using predefined message structures in a topic. Each of the nodes created

in ROS is an independent process which focuses on a single algorithm or task

reducing the complexity of the overall program.
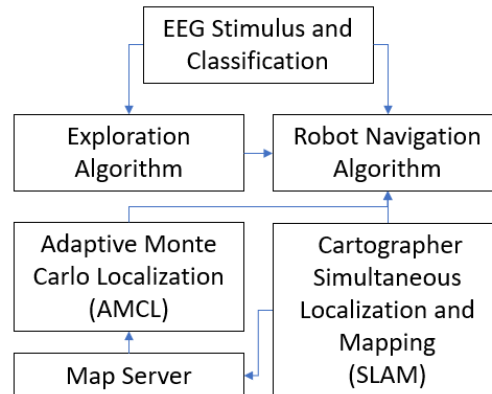
Figure 4.10   Block diagram of the software nodes developed in ROS for the
function of the autonomous wheelchair.

Toolsets and packages which were relevant and useful for the

application in this study were adapted and applied for use with the autonomous

wheelchair. These packages were implemented as nodes in ROS and could be

imported for use in this application. AMCL, Cartographer SLAM and Path

planners were implemented using the libraries from the existing toolbox. Three

new libraries -- EEG, wheelchair state, and exploration were developed in ROS

for the wheelchair to function. The EEG node contains the algorithm for

acquisition, classification, and stimulus generation. This node was created based

on the algorithm for BCI software described in Section 3.3. The robot state node

interacts with the differential drive robot controller described in Section 3.4.

The exploration node contains the algorithm for robot exploration described in

Section 3.4. Figure 4.10 shows the simplified block diagram of the developed

software nodes.

The wheelchair state node handles the data communication for the

wheelchair control board. Encoder, odometry and ultrasonics sensor information received from the wheelchair control board was published to ROS. This node is also responsible to take in velocity commands from the motion planner and forward it to the wheelchair control board driving the wheels of the wheelchair. Besides that, this node also published information regarding the location where all the sensors were mounted on the wheelchair.
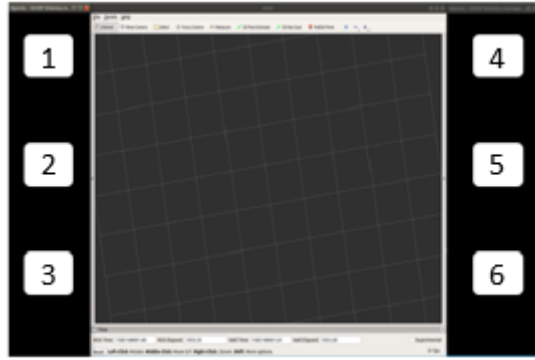
Figure 4.11   GUI developed for the control of the autonomous wheelchair. In the middle is the Robot Visualization (RViz) interface from the ROS framework. Six stimuli are placed on the left and right sides of the GUI, marked 1 to 6. Stimulus frequency for the boxes marked 1 to 6 are 7Hz, 11Hz, 12Hz, 13Hz, 14Hz, and 15Hz.

The EEG Node contains the classification algorithm, stimulus generation and handles the communication with the EEG acquisition unit for data acquisition. Figure 4.11 shows an example of the GUI developed for the wheelchair. A total of six stimuli for SSVEP are generated using OpenGL, 3 each on the left and right sides of the GUI. The algorithm described in Section 3.3 is implemented in this node. This node will generate a message when there is a successful SSVEP classification. The frequency used for the stimulus were 7Hz, 11Hz, 12Hz, 13Hz, 14Hz, and 15Hz.

The subject has the following two choices once the program starts: i) Directional Mode and ii) Destination mode. At the start of the program, the subject can select the mode of operation for the wheelchair. The directional mode will be triggered if a SSVEP corresponding to the stimulus on the left of the GUI is detected. Destination mode will be triggered if an SSVEP corresponding to stimulus 4, 5, or 6 is detected. Both directional and destination modes have the same interface as shown in Figure 4.11.

In directional mode, the subject will choose the direction of travel for the wheelchair. Successful SSVEP classification is used to trigger the direction of travel for the autonomous wheelchair. Only one input from the subject is needed to drive the wheelchair in this mode. The exploration algorithm will identify the waypoints for the wheelchair to travel. The path planner will plan the path and move towards the selected direction through the generated waypoints. SLAM will be running in this mode to record the map created over time. The subject can save any location in the map for use in destination mode.

Figure 4.11 shows the location and the frequency for each of the stimulus. Stimulus 1 will trigger the wheelchair to explore the front. Stimulus 2 will trigger the wheelchair to explore the back. Stimulus 4 will trigger the wheelchair to explore the left. Stimulus 5 will trigger the wheelchair to explore the right. The 4 quadrants directions are referenced to the current location of the wheelchair. Figure 4.12 shows an example of the four directions that the subject can select at any point of using the wheelchair. Stimulus 3 will stop the wheelchair if the wheelchair is exploring. If the wheelchair is not moving a trigger on stimulus 3 will bring the user back to the mode selection screen. Stimulus 6 will save the current location that can be used in the destination mode. A total of 16 location can be saved using directional mode.
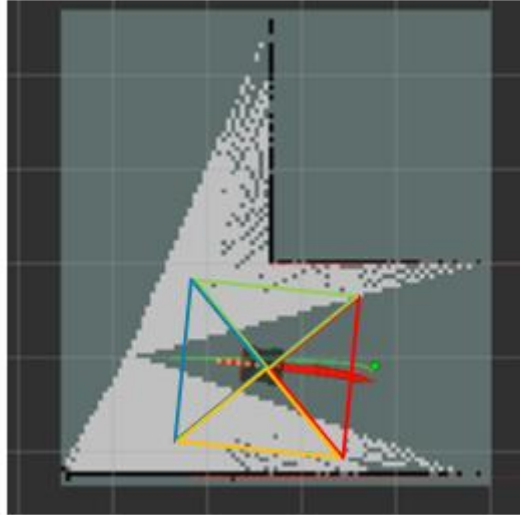
Figure 4.12   The 4 directions of travel for the wheelchair exploration to move to in directional mode. The red quadrant is front, blue is back, yellow is right and green is left.
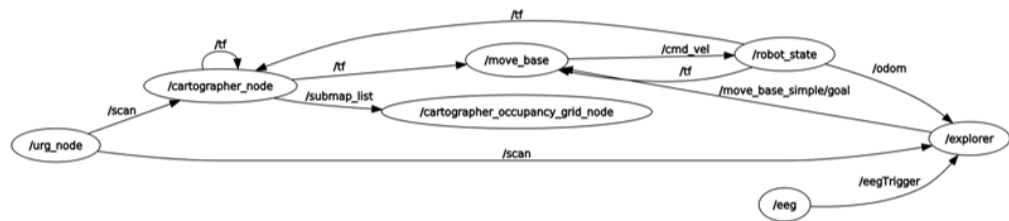
Figure 4.13   ROS node graph for the program when the wheelchair is operating in directional mode.

Once a direction of travel is triggered by the subject after SSVEP classification, the wheelchair will start to look for waypoints using the frontier algorithm as explained in Section 3.4.Figure 4.13 shows the nodes that are active in the directional node. Cartographer node contains the SLAM algorithm to generate the map of the surrounding. URG node is the node that publishes the sensor reading from the laser range finder. Robot state node is responsible for the wheelchair state and communication with the wheelchair control board. Move base node contains the algorithm for path planning and navigation. The EEG node includes the algorithm developed for the stimulus generation, acquisition, and classification of SSVEP. Lastly is the explorer node which

contains the exploration algorithm developed.
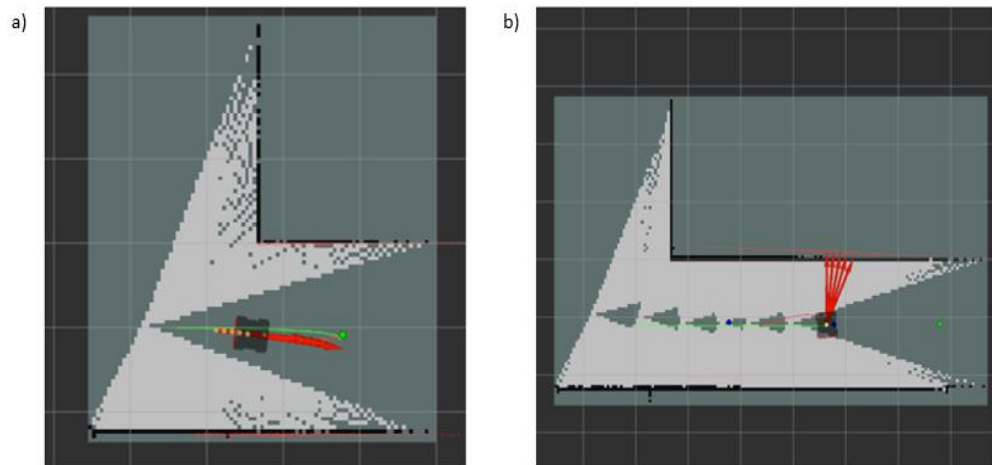
Figure 4.14   (a) Example of a wheelchair selected to explore in the front direction. The green dot in the figure shows the waypoint for the wheelchair to move towards. (b) The waypoint will be marked as explored and appear as blue in the map once the wheelchair passed the waypoint. New waypoints are generated automatically in the direction of travel selected.
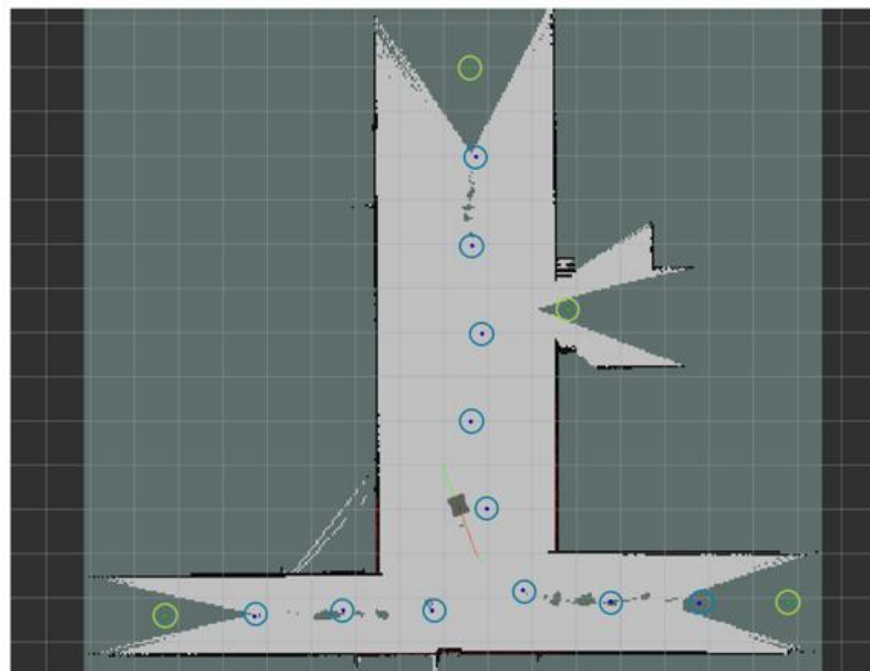
Figure 4.15   Example of a map generated after the wheelchair operated in the directional mode. Green waypoints in the map are located on parts where the map is still not explored. Blue waypoints in the map are waypoints where the wheelchair have explored.

Figure 4.14 shows an example of the exploration algorithm execution. In this example, the wheelchair is selected to move to the front. A waypoint marked as a green dot in Figure 4.14(a) is generated by the exploration algorithm. The green dot is located on an area where the map is not formed by SLAM. The wheelchair will proceed to move towards the waypoint generated in the direction of travel. The exploration algorithm will generate new waypoints while the wheelchair is moving. Figure 4.14(b) shows an example of a new waypoint generated while the wheelchair is moving forward in the direction of travel. These new waypoints that are generated will serve as the goals for the navigation algorithm in directional mode. Figure 4.15 shows the map and waypoints generated after the wheelchair is driven around using the directional mode. The directional mode allows the subject to move the wheelchair in the direction of travel with only one input provided.
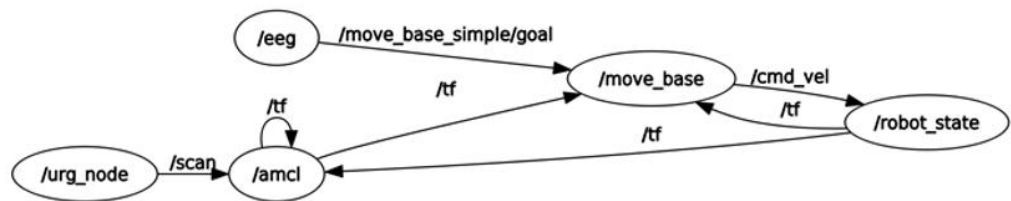
Figure 4.16   ROS node graph for the program when the wheelchair is operating in destination mode.

In the destination mode, the map generated, and location saved in the directional mode will be used for navigation. Figure 4.16 shows the nodes which are active in the destination mode. URG, move base, and robot state node are similar to the nodes created for the directional mode. Localization of the wheelchair in the map provided is performed by the AMCL node that runs the AMCL algorithm. On top of the task in the directional mode, the EEG node will

also send the coordinates of the selected location directly to the navigation algorithm in this mode.

Figure 4.11 shows the location of the stimulus of the GUI. The stimulus 1, 2, 4, and 5 are used for selection of destination to travel to. The target locations A, B, C, and D are tied to stimulus 1, 2, 4, and 5. Stimulus 3 will stop the wheelchair if the wheelchair is moving. If the wheelchair is not moving a trigger on stimulus 3 will bring the user back to mode selection. Stimulus 6 will cycle through the saved location, showing different sets of save location on the map shown in the GUI.
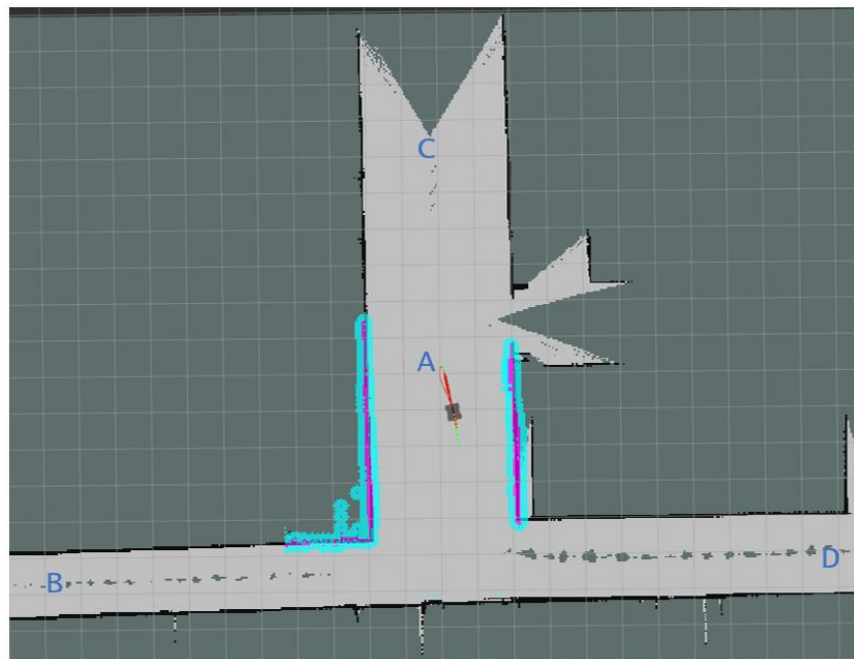
Figure 4.17   An example of the map shown to the subject in destination mode. Location A, B, C, and Dare the destinations where the subject can choose using SSVEP BCI.

Figure 4.17 shows the wheelchair navigating to position A on the map generated by SLAM. This map is obtained by SLAM when the wheelchair is operating in the directional mode. The wheelchair moves towards position A

following the path generated by the TEB path planner.

With both directional and destination modes, the wheelchair would be able to operate in an unknown environment, generating the map of the surrounding area using SLAM. After mapping, the subject on the wheelchair will be able to save destinations using SSVEP-based BCI to reduce the number of BCI tasks needed to move the wheelchair. By implementing these features for wheelchair control, the amount of input needed would be reduced for the navigation of the wheelchair. The next section will describe the result from the study conducted to measure the reduction of inputs for the control of an SSVEP-based BCI wheelchair.

4.5   Comparison between Distributed Control and Direct Control

Figure 4.18   Wheelchair configuration used for the comparison trial.

Figure 4.18 shows the wheelchair setup used for this study. The laser mounted at the front of the tray is used for SLAM and obstacle avoidance. A

2.2GHz Intel Core I5 laptop with 4GB RAM is used to run all the packages and algorithms created for the wheelchair. Five student volunteers were recruited to test the functionality of the wheelchair.
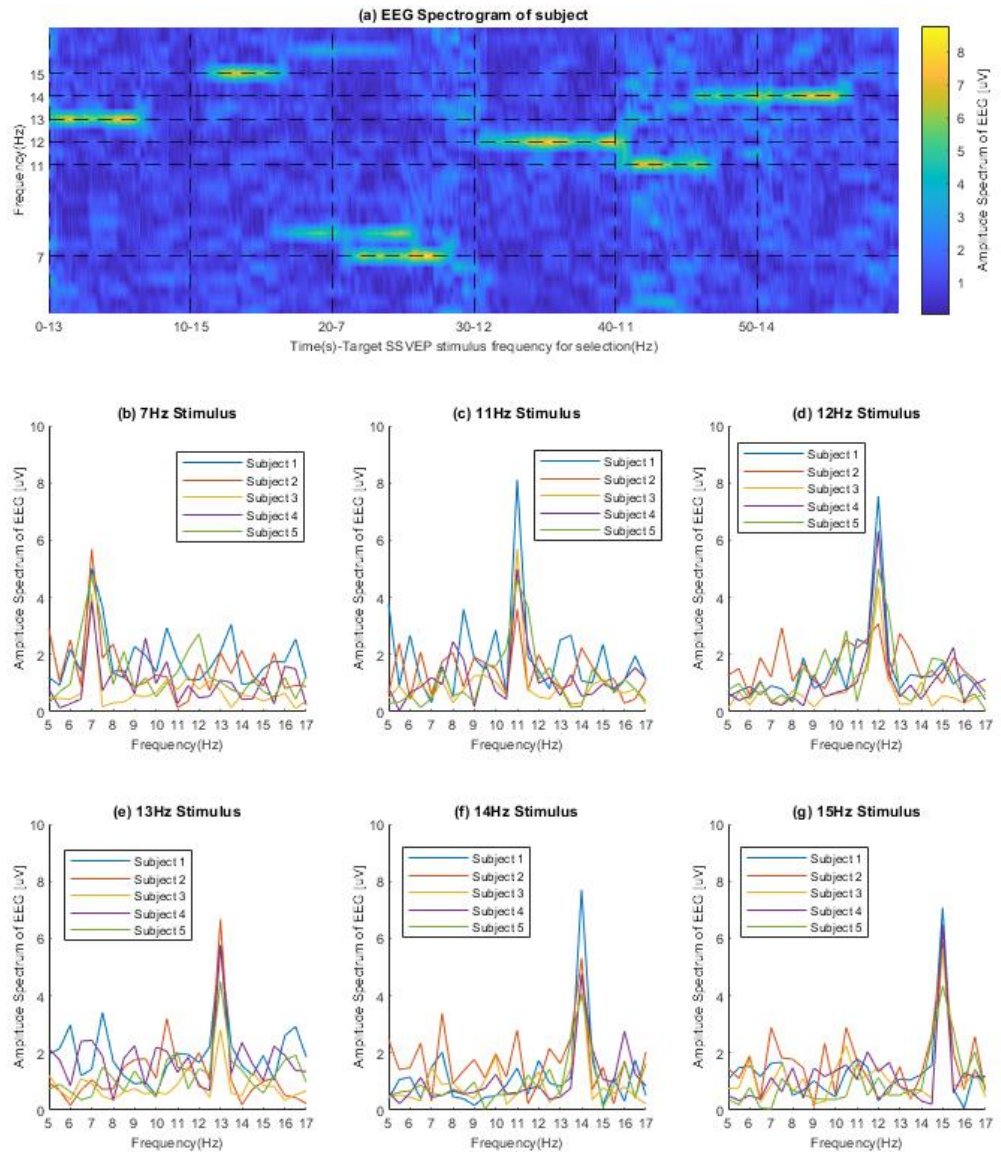
Figure 4.19   (a) EEG spectrogram showing SSVEP response of a subject to stimulus frequency in the order 13Hz, 15Hz, 7Hz, 12Hz, 11Hz, 14Hz during the training session.(b,c,d,e,f,g) Frequency components of the SSVEP measured at Oz for all 5 subjects during the training session. The stimulus frequencies are in the order 7Hz, 11Hz, 12Hz, 13Hz, 14Hz, and 15Hz.

A training for SSVEP selection was conducted to ensure that these five

student volunteers were familiar with the selection system before the trial with the wheelchair. The training required the subject to select the stimulus indicated by the interface when an arrow was shown beside the selection box. The training interface was similar to the training interface described in section 4.2. The subject was required to make 20 randomized selections for a single training session that lasted 4 hours. The subject would proceed to the wheelchair trial upon achieving a selection accuracy rate of at least 80%. Figure 4.19a shows the EEG spectrogram from one of the subjects. SSVEP responses can be observed when the subject is looking at the stimulus during training the training session. Figure 4.19b-g shows examples of SSVEP response measured on all 5 subjects during the training session.

Figure 4.20   The highlighted region indicates the area where the experiment was conducted. The blue dot on the map is the start position of the experiment. Green dots marked the 3 ends of the corridor in the experiment area.

After the completion of training, the subject proceeded with the wheelchair control trial. Figure 4.20 shows the layout of the area the test was conducted. The total area of the highlighted region is 157.9m^2. The distance to the three green dots from the starting position is 15.675m for the left, 23.925m for the top and 5.775m for the right. In this part of the study, 4 tasks were given to the subject. (1) Save the initial location of the wheelchair using the user interface. (2) Explore the test area to create a map of the corridor. (3) Navigate to the end of the corridor as shown in Figure 4.20. (4) Navigate back to the initial location using location saved in step 1. The theoretical minimum number of selections needed to complete the map and navigate the area indicated are 10 selections.

Table 4.3   Total number of SSVEP selections, time is taken, and accuracy for each of the subject to complete the wheelchair trial with directional and destination mode.

	Total Selection	Time Spent (Minutes:Seconds)	Accuracy (%)
Subject 1	15	16:10	93.33
Subject 2	16	17:20	93.75
Subject 3	15	16:45	100.00
Subject 4	18	18:32	83.33
Subject 5	19	20:40	78.95

Table 4.3 shows the number of total selections taken by the subject to complete the trial. The accuracy is calculated by taking the percentage of intended selections by the subject over total selections. Any selections by the subject to stop the wheelchair during directional or destination mode indicates that there is an unintended selection. Similarly, if the wheelchair is moving in a direction or destination that is not what the subject wanted to, it is also

considered an unintended selection. This definition of accuracy is taken to give the users the freedom for choosing their own pathways. Due to the accuracy in the selection and different approaches taken by the subject for step 2, the total number of selections is higher than the ideal case where 10 selections can complete the task given to them and thus the longer time spent to complete the trial. Despite having a higher number of selections, all the subjects managed to complete the trial given.

For comparison, an SSVEP-based BCI to control the wheelchair directly was implemented on the wheelchair developed. Four selections (forward, left, right, and stop) were used to control the motion of the wheelchair directly. The subject was required to explore the area similar to the wheelchair control trial using this control method. Table 4.4 shows the number of selections needed by the subject to fully explore the highlighted region and return to the initial location as shown in Figure 4.20. The accuracy was calculated by taking the percentage of the intended selection by the subject over the total selections. Any selections by the subject to stop the wheelchair within 2s after selecting forward left or right indicated that there was an unintended selection.

Table 4.4   Total number of SSVEP selections, time is taken, and accuracy for each of the subject to complete the wheelchair trial with direct (forward, left, right, and stop) controls.

	Total Selection	Time Spent (Minutes:Seconds)	Accuracy (%)
Subject 1	42	24:31	90.48
Subject 2	42	20:30	93.75
Subject 3	24	19:23	100.00
Subject 4	30	20:56	93.33
Subject 5	36	21:30	83.33

In the comparison trials, extra selections were taken by the subject to guide the wheelchair while navigating the corridor. More inputs from the user are required to control the wheelchair without the use of sensors for navigation. By delegating the navigational control task from the subject to the wheelchair, no constant BCI input is required when the wheelchair is navigating. The developed system required an average of 16.6 selections compare to a direct control system (Müller, et al., 2013) where an average of 32.8 selections was needed to complete the trial.

A smaller number of selections was needed in the developed system as no direct control of the wheelchair was required once a direction was selected. The navigation software acted as a distributed controller, controlling the wheelchair with information obtained from the laser range finder independent from the BCI system. The autonomous capabilities of the developed wheelchair allow for fewer inputs compared to a wheelchair system (Müller, et al., 2013; Wang & Bezerianos, 2017) which directly steers the wheelchair. This reduced the number of mental tasks required for a subject to control the wheelchair. With the dual-mode implementation of directional and destination controls, the

developed system would also overcome the problem of having only pre-set destinations for selection. In the real-world setting, the smaller number of selections is required to reduce the chances of false positive selection. This will reduce accidental triggering of the wheelchair by the user. If there is any false negative in the BCI system, the wheelchair will maintain its current state. Since the developed wheelchair has an autonomous navigation system, the wheelchair will navigate autonomously avoiding any danger while the user attempt to give new commands to the wheelchair.

The reduction in the inputs needed reduced the number of mental tasks required by the subject to operate the wheelchair (Ng & Goh, 2020). Similar to the shared-control BCI architectures for BCI control applications (Tonin et al., 2010; Chung et al. 2011 & Tang et al. 2017), the design developed in this study can reduce the number of BCI tasks needed to achieve a goal. One of the key features developed in this study is the EEG library node for SSVEP developed for ROS. This is a library that could help fastening any future developments that need to interface an EEG system with any robotic applications. A study for the use of this wheelchair on subjects with mobility impairments in the homecare settings was recently being conducted (Krishnan, et al., 2019). In the study, the subjects were able to command the wheelchair to move around in the compound of the homecare facility.

CHAPTER 5

CONCLUSION

5.1   Conclusion

In summary, a SSVEP-based BCI autonomous wheelchair with distributed controls that can function with minimal inputs from users was developed. By shifting the control task from the subject to an autonomous system, the system reduces the number of inputs required by a user to control the motion of the wheelchair. Once a selection is made in the directional mode, the wheelchair can continue to move in the direction selected without additional inputs. In destination mode, the wheelchair will move autonomously to the destination once a selection is made. The novelty of this study arises from the combination of techniques from autonomous robotics applications and BCI. A BCI wheelchair that can be operated with the least number of inputs has been developed.

One limitation of the current study is the cohort of the subject tested. All the subject volunteers that participated in the test were healthy undergraduate students. While the capability of the developed BCI wheelchair system was studied and tested, how does this result translate to the intended user group with mobility impairment is still unknown. Further studies should be conducted in the short term to address this limitation.

5.2   Future Direction

Studies to measure the effect of mental load and the quality of life of a subject using this wheelchair should be conducted. A preliminary study for the use of this wheelchair on subjects with mobility impairments in the home care settings was recently conducted (Krishnan, et al., 2019). More studies on subjects with severe mobility impairments using the wheelchair should be conducted. Results obtained from such studies are important to further improve the control scheme of the wheelchair.

Another direction for further studies is through the implementation of sensors and algorithm to enable the wheelchair to function outdoors. The algorithm created in this study needs to be expanded to cater for a wider area of operation and obstacle detection when operating outdoors. It is important to have both indoor and outdoor navigations for a person to fully regain the capability for mobility independence.

This study also demonstrated the use of robotics technology for BCI assistive technology. The application of robotics in BCI system is one of the directions that future research can embarked in. The control of telepresence robots or robotic arm using BCI is some examples of the area where the distributed approach developed in this study can be applied.

REFERENCES

Adrian, E.D. and Matthews, B.H.C., 1934. The berger rhythm: Potential changes from the occipital lobes in man. *Brain*, 57(4).

Allen, P.J., 2010. EEG instrumentation and safety. In: *EEG - fMRI: Physiological Basis, Technique, and Applications*.

Al-maqtari, M.T., Taha, Z. and Moghavvemi, M., 2009. Steady state-VEP based BCI for control gripping of a Robotic hand. *International Conference for Technical Postgraduates 2009, TECHPOS 2009*. 2009

Al-qaysi, Z.T., Zaidan, B.B., Zaidan, A.A. and Suzani, M.S., 2018. A review of disability EEG based wheelchair control system: Coherent taxonomy, open challenges and recommendations. *Computer Methods and Programs in Biomedicine*, 164.

Aurlien, H. et al., 2004. EEG background activity described by a large computerized database. *Clinical Neurophysiology*, 115(3).

Blankertz, B. et al., 2011. Single-trial analysis and classification of ERP components - A tutorial. *NeuroImage*, 56(2).

Boashash, B., 2015. *Time-Frequency Signal Analysis and Processing: A Comprehensive Reference*,

Bockbrader, M.A. et al., 2018. Brain Computer Interfaces in Rehabilitation Medicine. *PM and R*, 10(9).

Cao, T. et al., 2012. Flashing color on the performance of SSVEP-based brain-computer interfaces. *Proceedings of the Annual International Conference of the IEEE Engineering in Medicine and Biology Society, EMBS*. 2012

Chabuda, A. et al., 2019. Successful BCI communication via high-frequency SSVEP or visual, audio or tactile P300 in 30 tested volunteers. *Acta neurobiologiae experimentalis*, 79(4).

Chen, X. et al., 2018. Control of a 7-DOF Robotic Arm System with an SSVEP-Based BCI. *International Journal of Neural Systems*, 28(8).

Cheng, M., Gao, X., Gao, S. and Xu, D., 2002. Design and implementation of a brain-computer interface with high transfer rates. *IEEE Transactions on Biomedical Engineering*, 49(10).

Chin, S., 2017. *Effect of Age on Steady-State Visual Evoked Potential*.

Chung, M., Cheung, W., Scherer, R. and Rao, R.P.N., 2011. A hierarchical architecture for adaptive brain-computer interfacing. *IJCAI International Joint Conference on Artificial Intelligence*. 2011

Daubechies, I., 1990. The Wavelet Transform, Time-Frequency Localization and Signal Analysis. *IEEE Transactions on Information Theory*, 36(5).

Dehzangi, O. and Farooq, M., 2018. Portable Brain-Computer Interface for the Intensive Care Unit Patient Communication Using Subject-Dependent SSVEP Identification. *BioMed Research International*, 2018.

Diez, P.F. et al., 2013. Commanding a robotic wheelchair with a high-frequency steady-state visual evoked potential based brain-computer interface. *Medical Engineering and Physics*, 35(8).

Diez, P.F., Mut, V.A., Avila Perona, E.M. and Laciar Leber, E., 2011. Asynchronous BCI control using high-frequency SSVEP. *Journal of NeuroEngineering and Rehabilitation*, 8(1).

Do, A.H. et al., 2013. Brain-computer interface controlled robotic gait orthosis. *Journal of NeuroEngineering and Rehabilitation*, 10(1).

Faller, J., Müller-Putz, G., Schmalstieg, D. and Pfurtscheller, G., 2010. An application framework for controlling an avatar in a desktop-based virtual environment via a software SSVEP brain-computer interface. *Presence: Teleoperators and Virtual Environments*, 19(1).

Fan, T.L., Ng, C.S., Ng, J.Q. and Goh, S.Y., 2008. A brain-computer interface with intelligent distributed controller for wheelchair. *IFMBE Proceedings*. 2008

Ferguson, D., Likhachev, M. and Stentz, A., 2005. A guide to heuristic-based path planning. *Proceedings of the International Workshop on Planning under Uncertainty for Autonomous Systems, International Conference on Automated Planning and Scheduling (ICAPS)*.

Fernández-Rodríguez, Velasco-Álvarez, F. and Ron-Angevin, R., 2016. Review of real brain-controlled wheelchairs. *Journal of Neural Engineering*, 13(6).

Fifer, M.S. et al., 2013. Design and implementation of a human ECoG simulator for testing brain-machine interfaces. *International IEEE/EMBS Conference on Neural Engineering, NER*. 2013

Fox, D., 2003. Adapting the sample size in particle filters through KLD-sampling. *International Journal of Robotics Research*, 22(12).

Fox, D., Burgard, W. and Thrun, S., 1997. The dynamic window approach to collision avoidance. *IEEE Robotics and Automation Magazine*, 4(1).

Goh, S.Y. et al., 2005. A Brain-Computer Interface for control of a prosthetic hand. *Journal of Science and Technology in the Tropics*, 1, pp.35–41.

Grewal, H., Matthews, A., Tea, R. and George, K., 2017. LIDAR-based autonomous wheelchair. *SAS 2017 - 2017 IEEE Sensors Applications Symposium, Proceedings*. 2017

He, S. et al., 2017. A P300-Based Threshold-Free Brain Switch and Its Application in Wheelchair Control. *IEEE Transactions on Neural Systems and Rehabilitation Engineering*, 25(6).

Herrmann, C.S., 2001. Human EEG responses to 1-100 Hz flicker: Resonance phenomena in visual cortex and their potential correlation to cognitive phenomena. *Experimental Brain Research*, 137(3–4).

Hess, W., Kohler, D., Rapp, H. and Andor, D., 2016. Real-time loop closure in 2D LIDAR SLAM. *Proceedings - IEEE International Conference on Robotics and Automation*. 2016

Hwang, H.J. et al., 2012. Development of an SSVEP-based BCI spelling system adopting a QWERTY-style LED keyboard. *Journal of Neuroscience Methods*, 208(1).

Ito, T. et al., 2013. Design of brain-machine interface using near-infrared spectroscopy. *Journal of Robotics and Mechatronics*, 25(6).

Iturrate, I., Antelis, J.M., Kübler, A. and Minguez, J., 2009. A noninvasive brain-actuated wheelchair based on a P300 neurophysiological protocol and automated navigation. *IEEE Transactions on Robotics*, 25(3).

Khan, A.A., un Nabi, S.R. and Iqbal, J., 2013. Surface estimation of a pedestrian walk for outdoor use of power wheelchair based robot. *Life Science Journal*, 10(3).

Kishore, S. et al., 2014. Comparison of SSVEP BCI and eye tracking for controlling a humanoid robot in a social environment. *Presence: Teleoperators and Virtual Environments*, 23(3).

Koubaa, A. et al., 2018. Introduction to mobile robot path planning. In: *Studies in Computational Intelligence*.

Krishnan, K., Fan, T.L., Kiat, D.N.W. and Yau, G.S., 2019. Implementing a Brain-Computer Interface Wheelchair in Home-Care Setting: Preliminary Result. *Journal of Physics: Conference Series*. 2019

Kübler, A. et al., 2005. Severity of depressive symptoms and quality of life in patients with amyotrophic lateral sclerosis. *Neurorehabilitation and Neural Repair*, 19(3).

La Cruz, C., Bastos, T.F., Cheein, F.A.A. and Carelli, R., 2010. SLAM-based robotic wheelchair navigation system designed for confined spaces. *IEEE International Symposium on Industrial Electronics*. 2010

Lee, M.H. et al., 2019. EEG dataset and OpenBMI toolbox for three BCI paradigms: An investigation into BCI illiteracy. *GigaScience*, 8(5).
Leeb, R. et al., 2015. Towards independence: A BCI telepresence robot for

people with severe motor disabilities. *Proceedings of the IEEE*, 103(6).

Li, J. et al., 2014. Evaluation and application of a hybrid brain computer interface for real wheelchair parallel control with multi-degree of freedom. *International Journal of Neural Systems*, 24(4).

Li, Y. et al., 2011. Analysis of phase coding SSVEP based on canonical correlation analysis (CCA). *2011 5th International IEEE/EMBS Conference on Neural Engineering, NER 2011*. 2011

Li, Z., Xiong, Y. and Zhou, L., 2018. ROS-based indoor autonomous exploration and navigation wheelchair. *Proceedings - 2017 10th International Symposium on Computational Intelligence and Design, ISCID 2017*. 2018

Liu, Q., Chen, K., Ai, Q. and Xie, S.Q., 2014. Review: Recent development of signal processing algorithms for SSVEP-based brain computer interfaces. *Journal of Medical and Biological Engineering*, 34(4).

Lotte, F. et al., 2018. A review of classification algorithms for EEG-based brain-computer interfaces: A 10 year update. *Journal of Neural Engineering*, 15(3).

Mah, W.L., 2017. *A Steady-State Visual Evoked Potential-Based Brain Computer Interface System for Patients with Motor Disabilities*.

Mah, W.L. et al., 2019. SSVEP-based BCI for a DMD Patient - A Case Study. *2019 IEEE Conference on Sustainable Utilization and Development in Engineering and Technologies, CSUDET 2019*. 2019

Mandel, C. et al., 2009. Navigating a smart wheelchair with a brain-computer interface interpreting steady-state visual evoked potentials. *2009 IEEE/RSJ International Conference on Intelligent Robots and Systems, IROS 2009*. 2009

Millán, J.D.R. et al., 2009. Asynchronous non-invasive brain-actuated control of an intelligent wheelchair. *Proceedings of the 31st Annual International Conference of the IEEE Engineering in Medicine and Biology Society: Engineering the Future of Biomedicine, EMBC 2009*. 2009

Müller, S.M.T., Bastos, T.F. and Filho, M.S., 2013. Proposal of a SSVEP-BCI to command a robotic wheelchair. *Journal of Control, Automation and Electrical Systems*, 24(1–2).

Müller-Putz, G.R. and Pfurtscheller, G., 2008. Control of an electrical prosthesis with an SSVEP-based BCI. *IEEE Transactions on Biomedical Engineering*, 55(1).

Ng, D.W.K. and Goh, S.Y., 2020. Indirect control of an autonomous wheelchair using ssvep bci. *Journal of Robotics and Mechatronics*, 32(4).

Ng, D.W.K., Soh, Y.W. and Goh, S.Y., 2015. Development of an autonomous BCI wheelchair. *IEEE SSCI 2014 - 2014 IEEE Symposium Series on Computational Intelligence - CIBCI 2014: 2014 IEEE Symposium on*

Computational Intelligence in Brain Computer Interfaces, Proceedings. 2015

Ng, K.B., Bradley, A.P. and Cunnington, R., 2011. Effect of competing stimuli on SSVEP-based BCI. *Proceedings of the Annual International Conference of the IEEE Engineering in Medicine and Biology Society, EMBS*. 2011

Pfurtscheller, G. and Neuper, C., 2001. Motor imagery and direct brain-computer communication. *Proceedings of the IEEE*, 89(7).

Punsawad, Y. and Wongsawat, Y., 2013. Hybrid SSVEP-motion visual stimulus based BCI system for intelligent wheelchair. *Proceedings of the Annual International Conference of the IEEE Engineering in Medicine and Biology Society, EMBS*. 2013

Ramadan, R.A. and Vasilakos, A. v., 2017. Brain computer interface: control signals review. *Neurocomputing*, 223.

Ravanshad, N. and Rezaee-Dehsorkh, H., 2020. Level-crossing sampling: principles, circuits, and processing for healthcare applications. In: *Compressive Sensing in Healthcare*.

Rebsamen, B. et al., 2007. Controlling a wheelchair using a BCI with low information transfer rate. *2007 IEEE 10th International Conference on Rehabilitation Robotics, ICORR'07*. 2007

Rockey, C.A., Perko, E.M. and Newman, W.S., 2013. An evaluation of low-cost sensors for smart wheelchairs. *IEEE International Conference on Automation Science and Engineering*. 2013

Rosmann, C. et al., 2013. Efficient trajectory optimization using a sparse model. *2013 European Conference on Mobile Robots, ECMR 2013 - Conference Proceedings*. 2013

Sazgar, M. and Young, M.G., 2019. Overview of EEG, Electrode Placement, and Montages. In: *Absolute Epilepsy and EEG Rotation Review*.

Seo, S.P., Lee, M.H., Williamson, J. and Lee, S.W., 2019. Changes in Fatigue and EEG Amplitude during a Longtime Use of Brain-Computer Interface. *7th International Winter Conference on Brain-Computer Interface, BCI 2019*. 2019

Soh, Y.W., 2018. *Indirect Feedback Kalman Filter Based Sensor Fusion for Reducing Navigation Errors of an Autonomous Wheelchair*.

Soundarapandian, K. and Berarducci, M., 2009. Analog Front-End Design for ECG Systems Using Delta-Sigma ADCs. *System*, (March).

Sukerkar, K. et al., 2018. Smart Wheelchair: A Literature Review. *International Journal of Informatics and Communication Technology (IJ-ICT)*, 7(2).

Tanaka, K., Matsunaga, K. and Wang, H.O., 2005. Electroencephalogram-based

control of an electric wheelchair. *IEEE Transactions on Robotics*, 21(4).

Tang, J. and Zhou, Z., 2018. A shared-control based BCI system: For a robotic arm control. *1st International Conference on Electronics Instrumentation and Information Systems, EIIS 2017*. 2018

Teplan, M., 2002. Fundamentals of EEG measurement. *Measurement science review*, 2(2).

Texas Instruments, 2017. SDAS499C - ADS1299, ADS1299-4, ADS1299-6.

Thompson, M.C., 2019. Critiquing the Concept of BCI Illiteracy. *Science and Engineering Ethics*, 25(4).

Thrun, S., Fox, D., Burgard, W. and Dellaert, F., 2001. Robust Monte Carlo localization for mobile robots. *Artificial Intelligence*, 128(1–2).

Tonin, L. et al., 2010. The role of shared-control in BCI-based telepresence. *Conference Proceedings - IEEE International Conference on Systems, Man and Cybernetics*. 2010

Torkia, C. et al., 2015. Power wheelchair driving challenges in the community: A users' perspective. *Disability and Rehabilitation: Assistive Technology*, 10(3).

Tsubouchi, T., 2019. Introduction to simultaneous localization and mapping. *Journal of Robotics and Mechatronics*, 31(3).

Varona-Moya, S. et al., 2015. Wheelchair navigation with an audio-cued, two-class motor imagery-based brain-computer interface system. *International IEEE/EMBS Conference on Neural Engineering, NER*. 2015

Wang, H. and Bezerianos, A., 2017. Brain-controlled wheelchair controlled by sustained and brief motor imagery BCIs. *Electronics Letters*, 53(17).

Wang, H., Li, T. and Huang, Z., 2010. Remote control of an electrical car with SSVEP-Based BCI. *Proceedings 2010 IEEE International Conference on Information Theory and Information Security, ICITIS 2010*. 2010

Webster, J., 2010. Medical instrumentation: application and design, Fourth edition. *John Wiley and Sons, Inc. USA*.

Widmann, A., Schröger, E. and Maess, B., 2015. Digital filter design for electrophysiological data - a practical approach. *Journal of Neuroscience Methods*, 250.
Wilson, J.J. and Palaniappan, R., 2014. On the stimulus duty cycle in steady state visual evoked potential. *International Journal of Knowledge-Based and Intelligent Engineering Systems*, 18(2).

Wolpaw, J.R. et al., 2002. Brain-computer interfaces for communication and control. *Clinical Neurophysiology*, 113(6).

Wolpaw, J.R. et al., 2018. Independent home use of a brain-computer interface by people with amyotrophic lateral sclerosis. *Neurology*, 91(3).

Wu, C.H. and Lakany, H., 2013. The effect of the viewing distance of stimulus on SSVEP response for use in brain-computer interfaces. *Proceedings - 2013 IEEE International Conference on Systems, Man, and Cybernetics, SMC 2013*. 2013

Xie, J. et al., 2016. Effects of mental load and fatigue on steady-state evoked potential based brain computer interface tasks: A comparison of periodic flickering and motion-reversal based visual attention. *PLoS ONE*, 11(9).

Xu, Z., Li, J., Gu, R. and Xia, B., 2012. Steady-state visually evoked potential (SSVEP)-based brain-computer interface (BCI): A low-delayed asynchronous wheelchair control system. *Lecture Notes in Computer Science (including subseries Lecture Notes in Artificial Intelligence and Lecture Notes in Bioinformatics)*. 2012

Yamauchi, B., 1997. Frontier-based approach for autonomous exploration. *Proceedings of IEEE International Symposium on Computational Intelligence in Robotics and Automation, CIRA*. 1997

Yu, Y. et al., 2017. Toward a Hybrid BCI: Self-Paced Operation of a P300-based Speller by Merging a Motor Imagery-Based "Brain Switch" into a P300 Spelling Approach. *International Journal of Human-Computer Interaction*, 33(8).

Zhang, Z. et al., 2018. Design of an SSVEP-based BCI System with Vision Assisted Navigation Module for the Cooperative Control of Multiple Robots. *2017 IEEE 7th Annual International Conference on CYBER Technology in Automation, Control, and Intelligent Systems, CYBER 2017*. 2018

Zhang, Z. and Zhao, Z., 2014. A multiple mobile robots path planning algorithm based on a-star and dijkstra algorithm. *International Journal of Smart Home*, 8(3).

Zhu, D., Bieger, J., Garcia Molina, G. and Aarts, R.M., 2010. A survey of stimulation methods used in SSVEP-based BCIs. *Computational Intelligence and Neuroscience*, 2010.

INFORMED CONSENT FORM

Participant Name: _____ **I/C No**.: _____

Contact No.: _____ **Researcher Name**: _____

You are invited to participate in the following study. Your participation into this study is entirely voluntary. Your participation may not benefit you directly, but it will help us in improving the designs and operations of SSVEP-BCI system.

Title of Study: Trial of Brain-Computer Interface (BCI) controlled wheelchair using steady-state visual evoked potential (SSVEP)

Purpose of Study: To investigate the effectiveness of the SSVEP-BCI controlled wheelchair.

Procedures: First, the researchers will place some EEG electrodes at certain locations on the participant's scalp based on the International 10-20 system of EEG sensor placement. The researcher will check the SSVEP of participant when looking at a flickering patch or patches on a computer screen. After that, the researcher will guide the participant to use the SSVEP-BCI to control a wheelchair. The estimated duration for the experiment will last a maximum of 1.5 hours per trial including 30 minutes for setting up the EEG electrodes.

Page 1 of 3

Potential Risks:

There may be some discomfort experienced by attaching the electrodes on the scalp or skin with electro-gel and secured with stickers. Under rare circumstances, people with very sensitive skin may have some minor irritation or redness on the skin in reaction to the application of electro-gel.

The participant may find the experiment to be uncomfortable and unpleasant because of the duration of the experiment and the nature of the experiment that requires the participant has to look at the flickering patches on the computer screen.

The participant may also have eye fatigue after continually looking at the flickering stimuli over a long period.

Additionally, there is also a potential risk to induce cognitive side-effects including photo epileptic seizures by repetitive flickering stimuli modulated at certain frequencies.

The investigator will always check with the participant to determine if the participant is having any negative sensations during the experiment.

Confidentiality:

Information gathered from the study may be published or presented in public forums. However, your name and other identifying information will not be used or revealed.

Researcher's Signature: _____ **Date:** _____

Page 2 of 3

I have been fully informed and understood the above information. I have had the opportunity to discuss with the researcher and I have had my questions answered by him/her in a language that I understand. In signing this consent form, I agree to follow the procedures of the study, and I understand that my participation is voluntary, and I am free to withdraw my consent and discontinue my participation in this study at any time without any penalty.

I agree to take part in this study.

Participant's Signature: _____ **Date:** _____

Relationship to Participant: _____
(If other than participant giving consent)

Witness Name: _____ **Witness Signature:** _____

Page 3 of 3

APPENDIX B

UNIVERSITY ETHICAL APPROVAL

UNIVERSITI TUNKU ABDUL RAHMAN
Wholly Owned by UTAR Education Foundation (Company No. 578227-M)

Re: U/SERC/06/2016

15 January 2016

Prof Dato' Ir Dr Goh Sing Yau
Department of Mechanical and Material Engineering
Lee Kong Chian Faculty of Engineering and Science
Universiti Tunku Abdul Rahman
Jalan Sungai Long,
Bandar Sungai Long,
Cheras, 43000, Kajang,
Selangor

Dear Prof Goh,

Ethical Approval For Research Project/Protocol

We refer to your application dated 18 December 2015 for ethical approval for your research project and are pleased to inform you that your application has been approved under expedited review.

The details of your research project are as follows:

Research Title	To develop a pre-commercial prototype of a brain-computer interface (BCI) wheelchair
Investigator(s)	Prof Dato' Ir Dr Goh Sing Yau (PI)
	Dr Tan Lee Fan
	Mr Danny Ng Wee Kiat
	Ms Tan Yin Qing
	Prof Goh Khean Jin (UM)
	Prof Norlisah Mohd Ramli (UM)
	Mr Syed Putera bin Syed Mokhtar (Diesel Engineering Services Sdn Bhd)
Research Area	Science
Research Location	UTAR campus
No of Participants	20
Research Costs	MOSTI Flagship Project Research Grant
Approval Validity	2016 – 2017

The conduct of this research is subject to the following:

(1) The participants' informed consent be obtained prior to the commencement of the research.
(2) Confidentiality of participants' personal data must be maintained; and
(3) Compliance with procedures set out in related policies of UTAR such as the UTAR Research Ethics and Code of Conduct, Code of Practice for Research Involving Humans and other related policies/guidelines.

Address: Jalan Sg. Long, Bandar Sg. Long, Cheras, 43000 Kajang, Selangor D.E. Postal Address: P O Box 11384, 50744 Kuala Lumpur, Malaysia
Tel: (603) 9086 0288 Fax: (603) 9019 8868 Homepage: http://www.utar.edu.my

Should you collect personal data of participants in your study, please have the participants in the research signed the attached Personal Data Protection Statement for your records.

The University wishes you all the best in your research.

Thank you.

Yours sincerely,
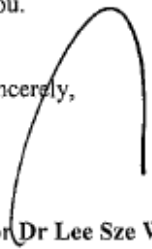
Professor Dr Lee Sze Wei
Chairman
UTAR Scientific and Ethical Review Committee

c.c   Dean, Lee Kong Chian Faculty of Engineering and Science
       Director, Institute of Postgraduate Studies and Research

APPENDIX C

EEG ACQUISITION UNIT BILL OF MATERIALS

Part	Value	Device	Package
C1	4.7n	C-USC0603K	C0603K
C2	4.7n	C-USC0603K	C0603K
C3	4.7n	C-USC0603K	C0603K
C4	4.7n	C-USC0603K	C0603K
C5	4.7n	C-USC0603K	C0603K
C6	4.7n	C-USC0603K	C0603K
C7	4.7n	C-USC0603K	C0603K
C8	4.7n	C-USC0603K	C0603K
C9	4.7n	C-USC0603K	C0603K
C10	4.7n	C-USC0603K	C0603K
C11	4.7n	C-USC0603K	C0603K
C12	4.7n	C-USC0603K	C0603K
C13	4.7n	C-USC0603K	C0603K
C14	4.7n	C-USC0603K	C0603K
C15	4.7n	C-USC0603K	C0603K
C16	4.7n	C-USC0603K	C0603K
C17	1u	C-USC0603K	C0603K
C18	1u	C-USC0603K	C0603K
C19	0.01u	C-USC0603K	C0603K
C20	0.1u	C-USC0603K	C0603K
C21	1u	C-USC0603K	C0603K
C22	0.1u	C-USC0603K	C0603K
C23	1u	C-USC0603K	C0603K
C24	1u	C-USC0603K	C0603K
C25	100u	C-USC1210K	C1210K
C26	1u	C-USC0603K	C0603K
C27	10u	C-USC0805K	C0805K
C28	0.1u	C-USC0603K	C0603K
C29	10u	C-USC0805K	C0805K
C30	10u	C-USC0805K	C0805K
C31	0.1u	C-USC0603K	C0603K
C32	10u	C-USC0805K	C0805K
C33	1u	C-USC0603K	C0603K
C34	1u	C-USC0603K	C0603K
C35	0.1u	C-USC0603K	C0603K
C36	0.1u	C-USC0603K	C0603K
C37	0.1u	C-USC0603K	C0603K
C38	0.1u	C-USC0603K	C0603K
IC1	ADS1299IPAG	ADS1299IPAG	TQFP64-10X10
IC2	OPA376	OPA376AIDBVTG4	SOT23-5
IC3	OPA376	OPA376AIDBVTG4	SOT23-5
IC4	PIC24FJ64GB004	PIC24FJ64GB004	TQFP44
IC5	MCP1700	MCP1700	SOT23
L1	3.3u	R-US_R0805	R0805

Part	Value	Device	Package
R1	4.99k	R-US_R0603	R0603
R2	4.99k	R-US_R0603	R0603
R3	4.99k	R-US_R0603	R0603
R4	4.99k	R-US_R0603	R0603
R5	4.99k	R-US_R0603	R0603
R6	4.99k	R-US_R0603	R0603
R7	4.99k	R-US_R0603	R0603
R8	4.99k	R-US_R0603	R0603
R9	4.99k	R-US_R0603	R0603
R10	4.99k	R-US_R0603	R0603
R11	4.99k	R-US_R0603	R0603
R12	4.99k	R-US_R0603	R0603
R13	4.99k	R-US_R0603	R0603
R14	4.99k	R-US_R0603	R0603
R15	4.99k	R-US_R0603	R0603
R16	4.99k	R-US_R0603	R0603
R17	2M	R-US_R0603	R0603
R18	2M	R-US_R0603	R0603
R19	392k	R-US_R0603	R0603
R20	10k	R-US_R0603	R0603
R21	10k	R-US_R0603	R0603
R22	10k	R-US_R0603	R0603
R23	10k	R-US_R0603	R0603
R24	10k	R-US_R0603	R0603
SV1		MA08-1	MA08-1
SV2		MA10-1	MA10-1
SV3		MA05-1	MA05-1
X2	USBSMD	USBSMD	USB-MINIB